

FINAL TECHNICAL REPORT

Project Title: Industrial Energy Conservation, Forced Internal Recirculation Burner
Covering Period: March 1, 1995 through December 31, 2001
Awardee: Gas Technology Institute
1700 South Mount Prospect Road
Des Plaines, IL 60018
Award Number: DE-FC07-95ID13333 (GTI Project No. 61107)
Limitations: None
Subcontractors: Detroit Stoker Company, Incorporated
Gas Institute of Ukraine
University of Illinois at Chicago
Other Partners: Southern California Brewery (identity confidential)
Project Director: Joseph Rabovitser, (847) 768-0548.
joseph.rabovitser@gastechnology.org
Project Objective: The overall objective of this research project is to develop and evaluate an industrial low NO_x burner for existing and new gas-fired combustion systems for intermediate temperature (1400° to 2000°F) industrial heating devices such as watertube boilers and process fluid heaters.

A multi-phase effort is being pursued with decision points to determine advisability of continuance. The current contract covers Phases II and III of this work. The objectives of each phase are as follows.

Phase II – to design, fabricate, and evaluate prototype burners based on the Forced Internal Recirculation (FIR) concept.

Phase III – to evaluate the performance of an FIR burner under actual operating conditions in a full-scale field test and establish the performance necessary for subsequent commercialization.

DISCLAIMER:

This report was prepared as an account of work supported by the U.S. Department of Energy under Award No. DE-FC07-95ID13333, GRI, and GTI's Sustaining Membership Program. Neither the U.S. Department of Energy, GRI, GTI, nor any of their employees, contractors, sub-contractors, or their employees makes any warranties, expressed or implied, or assumes any legal liability or responsibility for the accuracy, completeness, or usefulness of any information, apparatus, project, or process disclosed, or represents that its use would not infringe privately owned rights.

Reference to trade names or specific commercial products, commodities, or services in this report does not represent or constitute an endorsement, recommendation, or opinion of suitability by the U.S. Department of Energy, GRI, or GTI of the specific commercial product, commodity, or service.

Executive Summary

This project is intended to develop and field test an advanced industrial ultra-low-NO_x burner for existing and new gas-fired combustion systems applied to intermediate-temperature (1400° to 2000°F) industrial heating devices such as watertube boilers and process fluid heaters. It is an extension of a Phase I effort to develop the Forced Internal Recirculation (FIR) burner. Phase II includes the design, fabrication, and evaluation of prototype burners, and Phase III consists of full-scale field-testing of an FIR burner on an industrial watertube boiler.

The FIR burner is unique in its ability to deliver ultra-low-NO_x performance on watertube boilers without the use of external flue gas recirculation (FGR) or other energy-robbing approaches such as very high excess air or steam injection. The FIR burner allows industrial plants to meet the most stringent regional air emissions regulations at higher energy efficiency than possible with competing technology.

Three FIR burners were tested under this project: a 6-million-Btu/h laboratory burner, a 20-million-Btu/h prototype at a Detroit Stoker Company manufacturing facility, and a 60-million-Btu/h commercial prototype at a brewery in southern California. NO_x emissions* in the range of 6 to 9 vppm were achieved in all cases with low CO emissions, 4:1 turndown, and excellent flame stability. An improvement in boiler efficiency of approximately 1% was also confirmed for the 60-million-Btu/h commercial prototype, which was subsequently purchased by the host site for baseload steam generation.

The FIR burner benefits the public by simultaneously addressing the problems of air pollution and energy conservation through an ultra-low-NO_x combustion technology that does not increase energy consumption. Continuing activities include the negotiation of a license with Coen Company, Incorporated to commercialize the FIR burner for industrial package watertube boilers, and the development of a 5-vppm-NO_x version of the burner to meet anticipated future air quality regulations.

Objectives

The overall objective of this research project is to develop and field test an industrial ultra-low-NO_x burner for existing and new gas-fired combustion systems applied to intermediate-temperature (1400° to 2000°F) industrial heating devices such as watertube boilers and process fluid heaters.

A multi-phase effort is being pursued with decision points to determine advisability of continuance. The current contract covers Phases II and III of this work. The objectives of each phase are as follows.

Phase II – to design, fabricate, and evaluate prototype burners based on the Forced Internal Recirculation (FIR) concept.

* All emissions are corrected to 3% oxygen by volume.

Phase III – to evaluate the performance of an FIR burner under actual operating conditions in a full-scale field test and establish the performance necessary for subsequent commercialization.

Accomplishments

In Phase II, ultra-low-NO_x FIR burners were designed, built, and evaluated. A 6-million-Btu/h laboratory burner was extensively studied on a boiler simulator, and a 20-million-Btu/h prototype was designed, built, and studied on a watertube boiler at Detroit Stoker Company (DSC). In both cases, NO_x emissions in the range of 6 to 9 vppm were achieved with low CO emissions, 4:1 turndown, and excellent flame stability.

In Phase III, a 60-million-Btu/h FIR burner was designed, built, and installed on a working industrial watertube boiler in southern California. The burner was subjected to full-scale field tests, demonstrating NO_x emissions consistently below 9 vppm. The host brewery has purchased the burner and, at this writing, is using it for baseload steam generation in their manufacturing facility.

Based on this successful Phase III performance, a license for the FIR burner was negotiated with Coen Company, Incorporated (Coen) for watertube boilers up to 250 million Btu/h. Coen is one of the largest U.S. manufacturers of combustion equipment for boilers and process heaters, and has stated their intention to aggressively commercialize the FIR burner. Coen has also joined the project team as a subcontractor to participate in the development and field evaluation of a 5-vppm-NO_x version of the FIR burner.

FIR burner development and field evaluation will continue with funding from the natural gas industry and Coen. Ongoing work includes the design and fabrication of a 20-million-Btu/h 5-vppm-NO_x FIR burner to be tested on a watertube boiler at the GTI laboratories and a 50-million-Btu/h FIR burner that will be demonstrated at a host site in southern California. The 50-million-Btu/h burner will be tested in both 9- and 5-vppm-NO_x configurations. These demonstrations will lead to the commercialization of an entire line of FIR burners for watertube boilers in various markets depending on the regional NO_x requirements.

Background

The FIR burner has been under development since 1992 to address the need for a simple, cost-effective alternative to current approaches for NO_x control from gas-fired boilers and process heaters. In current practice, low-NO_x burners are used in combination with flue gas recirculation (FGR) to reach compliance NO_x levels. Tailpipe emissions controls such as SCR are required to reach even lower (<10 vppm) NO_x emissions required in some areas. But FGR presents problems including the need for additional equipment, more complex controls, reduced responsiveness, and higher operating costs. SCR presents additional problems with cost of buying and handling chemicals and further constrains the operability of the boiler. The FIR burner is designed to suppress NO_x formation to very low levels without resorting to external FGR or tailpipe chemical injection, using a simple approach based on a burner design as shown in Figure 1.

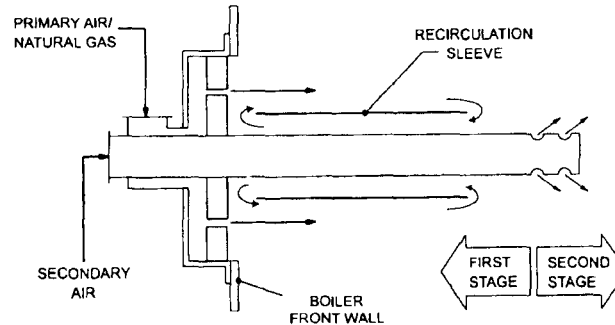


Figure 1. Forced Internal Recirculation Burner

The FIR burner uses air staging or fuel-air staging and a unique recirculation sleeve or insert to distribute the heat release, radiate a substantial portion of heat to the boiler walls, and induce the recirculation of partial combustion products from the end of the first stage back to the root of the flame. The flame is also arrayed in a ring around the central axis to further distribute the heat release and eliminate high-temperature zones that raise NO_x levels.

Task-by-Task Discussion of Results

Phase II. Prototype Development

Task II-1. National Environmental Policy Act

This project received a categorical exclusion for this Task.

Task II-2. Laboratory Evaluation

Based on experimental data generated on the 6-million-Btu/h flexible test burner at GTI, a 20-million-Btu/h commercial prototype burner was designed by GTI and DSC. The prototype burner is a scaled-up version of the air-staged laboratory burner. It was designed with adjustable geometry to evaluate key design parameters including: (1) distance between recirculation insert and primary nozzle plane, (2) distance between recirculation insert and secondary air tip, (3) secondary air velocity, (4) effect of tertiary air, (5) primary air velocity, and (6) recirculation insert length.

The burner was installed on a 20-million-Btu/h boiler at DSC's manufacturing facility in Monroe, Michigan. The host boiler, originally a stoker that was converted to natural gas firing before the beginning of this project, is used for process steam and for heating the 400,000-square-foot

manufacturing facility during the winter months. The existing burner controls were interfaced with the FIR prototype burner for testing. Water-cooled panels were installed over the refractory floor at the beginning of the project to determine the effect of cooling surface on emissions. A photograph of the burner installed at the host site is shown in Figure 2.

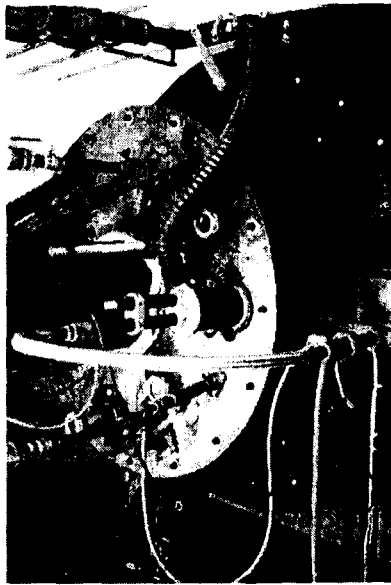


Figure 2. 20-million-Btu/h Prototype FIR Burner on DSC Boiler

The major measurements included primary air, secondary air, natural gas, and cooling water flow rates; appropriate temperature measurements to approximate the heat flux profile along the combustion chamber length; and NO/NO_x, O₂, CO, CO₂, and THC (total hydrocarbon) emissions in the primary zone and exhaust gas, as well as exhaust gas temperature.

Exhaust gas samples were drawn through a 3/4-inch-OD by 4-foot-long, water-cooled probe using oil-less vacuum pumps and sample conditioning trains, which consist of two water traps, a membrane dryer, and a final water trap to ensure that the sample is dry before entering the on-line emission monitors. A stream switching panel is used to facilitate easy switching between gas sampling and instrument calibration. The combustion products were analyzed using the following continuous gas monitors:

- A ThermoElectron Model 14A chemiluminescence NO_x analyzer
- A Rosemount Analytical Model 880A infrared carbon monoxide analyzer
- A Beckman Model 400 flame ionization total hydrocarbons analyzer

- A Rosemount Analytical Model 755R paramagnetic oxygen analyzer
- A Rosemount Analytical Model 880A infrared carbon dioxide analyzer.

Pure nitrogen was used as a zero gas, and individual span gases were used to calibrate each instrument. Each span gas consisted of the individual component (O₂, CO, etc.) in nitrogen.

Testing began in September 1997, and burner variations in operational and geometrical burner parameters were evaluated. Operational parameters included the distribution of primary and secondary air, load changes, lower load at higher primary air, and pilot conditions. Geometrical burner parameters that were evaluated included means for changing the secondary/tertiary air ratio, the distance between the recirculation insert and the nozzles, the distance between the recirculation insert and the secondary air tip, and the secondary air open area.

Two test campaigns were conducted:

- FIR burner/water-cooled floor – starting in 1997, the boiler included water-cooled panels on the floor, resulting in approximately 80% internal wall coverage by a cooling surface;
- FIR burner/refractory floor – prior to the 1998 heating season, the boiler was prepared for continuous operation without the water-cooled panels on the floor (refractory floor). This resulted in approximately 60% internal wall coverage by a cooling surface.

Data from testing at DSC are summarized in Table 1.

Table 1. Data from 20-million-Btu/h Prototype Burner at DSC Facility

	Water-cooled Floor			Refractory Floor		
Firing Rate, million Btu/h	5	11	20	11	15	19
Load, %	25	55	100	55	75	95
O ₂ , %	3.0	2.5	2.9	3.0	2.8	2.1
NO _x , vppm	8.3	6.7	7.2	8.0	9.9	8.6
CO, vppm	40	18	3	10	19	11

With the water-cooled floor, NO_x concentrations ranged from 6.7 vppm at 11 million Btu/h to 8.3 vppm at 5 million Btu/h. Excess air in the stack ranged from 14.9% to 12.1% (3.0% to 2.5% O₂) and maximum CO emissions were 40 vppm, measured at 25% load. Additional tests were performed which included automatic start up and operation, load swinging from 20 to 100% at regular and increased speed, and boiler shut down.

With the refractory floor, NO_x concentrations ranged from 8.0 vppm at 11 million Btu/h to 9.9 vppm at 15 million Btu/h, but with a slightly lower value at maximum fire. It was not possible to test at lower loads since steam was required for heating and manufacturing use. Excess air in the stack ranged from 14.9% to 10.0% (3.0% to 2.1% O₂) and CO emissions were consistently below 25 vppm. As were conducted earlier, additional tests were performed which included

automatic start up and operation, load swinging from 55 to 100% at regular and increased speed, and boiler shut down.

The FIR burner has been in operation for over four years on the unattended watertube boiler at DSC, and has logged over 10,000 hours. Overall, the burner has experienced high reliability with no deterioration of performance. Currently, the DSC burner has been removed because the boiler is being used to test a backup oil-fired burner required at the facility. There have been no problems with the FIR burner, but the DSC facility does not require low-NO_x operation and so does not incur any penalty by removing the burner from service to free up the boiler for other testing.

Task II-3. Modeling Work

A computer model written earlier for firetube boilers was modified to accommodate the watertube boiler configuration (rectangular combustion chamber and combustion gases passing through a 90 degree turn), different conditions for heat and mass transfer, NO_x formation, and an increased (scaled-up) firing rate. The Gas Institute of Ukraine performed calculations combining fluid dynamics, heat transfer, and combustion chemistry. A Digest of their findings was submitted to GTI.

FLUENT® CFD code was also used for assisting design calculations for the 60-million-Btu/h commercial prototype burner in southern California. The burner was originally designed in an air-staging configuration with a conical secondary air distributor.

The physical models utilized in the calculations are presented below in Table 2.

Table 2. Physical Models Used for CFD Calculations

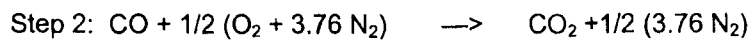
Model	Settings
Space	3D
Time	Steady
Viscous	Standard k-epsilon turbulence model
Wall Treatment	Standard Wall Functions
Heat Transfer	Enabled
Radiation	P1 Model
Species Transport	Reacting (6 species)

The chemistry model was developed based on current experimental and theoretical understanding of cool flame chemistry. The main postulates of the model are as follows:

- Cool flame oxidation of methane can occur at temperatures about 1100°F and proceeds at a low rate (characteristic time 0.01-0.10 seconds) compared to regular high temperature flames;

- The oxidation rate is lower than the rate of turbulent energy transfer, which results in fast energy removal from the energy release zone.

The influence of turbulence on the reaction rate is modeled using the eddy-dissipation model of Magnussen and Hjertager. The Arrhenius reaction rates were combined with the eddy-dissipation model reaction rates (adjusted to provide postulated interaction between chemical reaction and turbulent mixing). The parameters of the model were fit based on the test results of the 20-million-Btu/h DSC burner. The following two-step chemistry model, representing the combustion of methane in air, was implemented:



Radiative heat transfer within the burner was modeled using the P-1 radiation model in FLUENT[®]. Turbulent flow simulations were performed using the standard two equation k-ε model of Fluent with the standard wall functions. Default settings in FLUENT[®] were used for turbulence model settings.

The CFD mesh was built based on the current understanding of the modeled flame. A fine mesh was built for the fuel inlet jets area, the beginning and the end of the recirculation sleeve, and the secondary flame zone. Special attention was given to the recirculation sleeve surface area. The mesh was built in such way to keep y+ values around 30 near the surface. The adaptation of the mesh near the sleeve surface fuel inlets and secondary air inlet was carried out during the solution.

Physical properties of the gases involved (heat capacity and conductivity) were computed from mixture rules for species dependence. The heat capacity of the mixture was assumed to be a function of temperature using the polynomial fit. The density of the mixture was changed to an incompressible ideal gas, *i.e.*, the density changes as a function of temperature and species concentrations, and the variability with pressure was ignored. The molecular viscosity was chosen to be a constant.

The boundary conditions used in the analysis were derived from engineering study of the host boiler.

Geometrical changes that were varied for different cases are listed below:

- Primary nozzle diameter (uniform nozzles)
- Recirculation sleeve diameter
- Primary nozzle diameters (non-uniform nozzles)
- Symmetrical versus asymmetrical primary nozzle distribution
- Secondary air distribution (conical slit versus individual nozzles)

Results of the modeling showed that: NO_x is mostly produced in hot zones in the second stage of the flame (average 90% of the total NO_x production). Flame analysis showed three possible ways to decrease local peak temperatures:

- Promote more uniform mixing of the first-stage gases by tailoring the arrangement of primary nozzles to the combustion chamber profile and aspect ratio;
- Injecting secondary air in an array of single jets instead of a cone-shaped planar jet as originally planned; Figure 3 shows the presence of hot spots in the shadow of the conical distributor;
- Increasing the proportion of heat release from the primary zone, thus reducing the flame temperature of second-stage combustion.

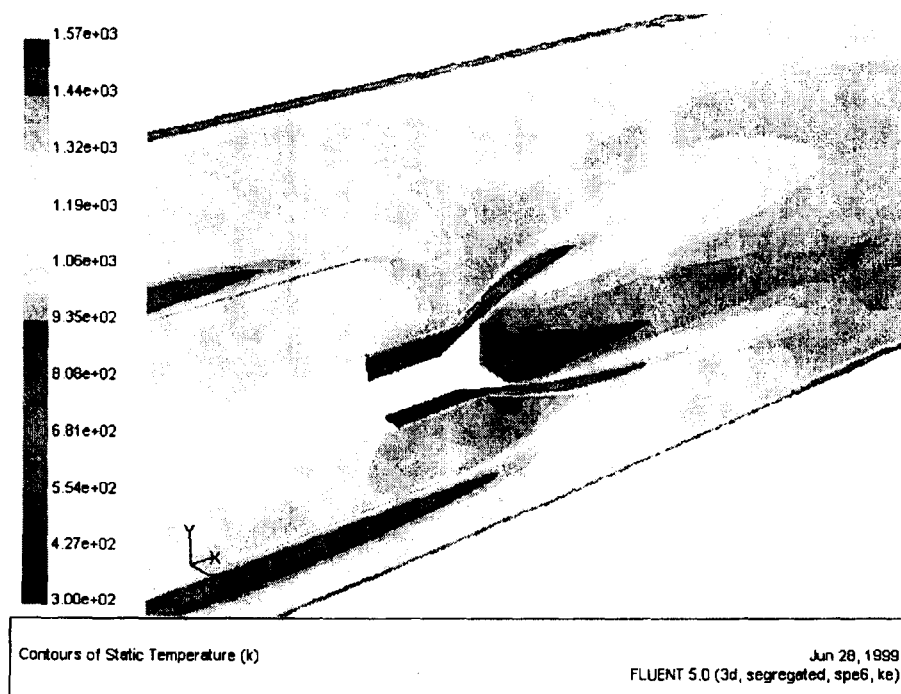


Figure 3. CFD Model Representation of Temperature Distribution in the Secondary Flame

CFD model calculations suggested several modifications that could reduce NO_x emissions by a factor of two without making gross changes to the burner geometry. The modeling results show that optimization of the current design of the burner could include the optimization of nozzles size/location in order to fit the flame to the combustion chamber, and optimization of the secondary air injection.

The model was validated based on the test results of the DSC burner flame. The model parameters for flame chemistry, turbulence and mesh were fit in order to provide an agreement with measured profiles of temperature and concentrations of CO₂, O₂ and THC in the DSC flame.

The results of the CFD modeling were applied to the design of the 60-million-Btu/h burner, which resulted in a faster transition from initial installation to demonstrated attainment of performance targets.

Task II-5. Study of NO/NO₂ Formation

This Task was added to accommodate a detailed study of unusual NO/NO₂ ratios in the primary zone under many test conditions at the DSC facility. Specifically, up to 90% of primary zone NO_x was in the form of NO₂, which accounted for more than 60% of total NO_x. This is in contrast to typical NO_x production in natural gas flames where NO₂ accounts for less than 10% of total NO_x. Typical data from a test in 1999 is shown in Figure 4, where NO₂ varies from 68% to 98% of total NO_x, depending on the location in the primary combustion zone. This test was conducted at 15 million Btu/h (75% load) with a primary stoichiometric ratio of 0.65 and 15% total excess air. NO_x at the boiler exit was 6.3 vppm, of which 40% was NO₂.

To clarify this behavior and obtain data for further modeling and analysis of chemical kinetics, the 6-million-Btu/h laboratory FIR burner was prepared for detailed primary zone testing. Three different configurations were evaluated on the GTI boiler simulator. Emphasis was placed on characterization of the primary zone and the related NO₂ values. NO_x concentrations ranged from near zero to 6 vppm, but the NO₂ fraction was significant (>10% of total NO_x) at certain conditions. Figure 5 shows data from the air-staging configuration with varying secondary-to-primary air ratios. The firing rate was 4 million Btu/h (75% load) with a primary stoichiometry of 0.74 and overall excess air ranging from 12% down to -18% (substoichiometric). NO_x at the boiler simulator exit was 7 to 10 vppm, of which 20% was NO₂.

The level of NO₂ in the primary zone was much lower and the shift from NO₂ to NO occurred faster and more completely in the laboratory burner. However, there are similarities in the pattern of NO_x proportioning between NO and NO₂ between the laboratory and the DSC burner, as evident from the peak in NO₂ content that occurs in both cases at the secondary combustion zone.

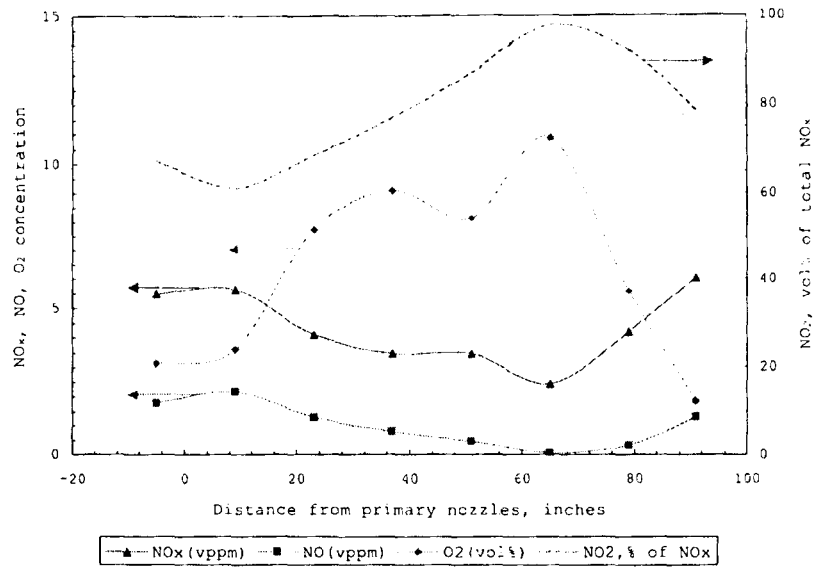


Figure 4. Typical NO_x Distribution in Primary Zone of DSC Burner

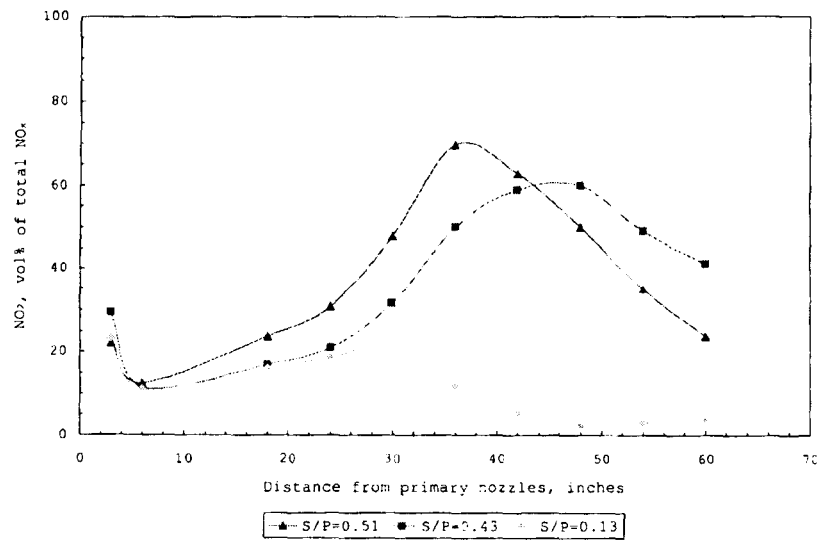


Figure 5. NO_2 in Primary Zone of Laboratory Burner versus Air Staging

A study of NO_x formation mechanisms with the goal of explaining the high NO₂ content in certain regions of the FIR burner was subcontracted to the University of Illinois at Chicago (UIC) Mechanical Engineering department. A report was submitted to GTI in January 1999, and a copy is available on request. The conclusion of this study was that low NO_x levels combined with high NO₂ content in the FIR burner flue gases resulted from a pathway which involved high HO₂ concentrations in the rich premixed flame. The predicted reaction path of NO_x formation proceeds through reactions between molecular nitrogen and CH radicals, which in turn are characteristic of a "cool" flame with long-lived intermediate radicals and molecules due to processes of turbulent mixing and recirculation.

Phase III. Field Evaluation

Task III-3. Commercial Burner Design

The results of laboratory testing in Phase II were used to optimize the design of a commercial burner based on the actual boiler capacity and design at a selected host site (see Task III-4 below). A detailed design package was prepared and released for fabrication.

Task III-4. Host Site Identification and Selection

A field demonstration prospectus was developed and distributed to potential host sites. A brewery in southern California was selected as a suitable host site for commercial prototype burner testing, and the project team developed installation drawings based upon the host site's particular requirements. Site permitting was initiated, a Field Experiment Agreement among GTI, DSC, and the host site was finalized, and interface drawings were prepared. A permit application for the host boiler retrofit was submitted to the South Coast Air Quality Management District in July 1998, and formal notification of the granting of an experimental research permit was received in November 1998.

Task III-5. Commercial Burner Testing

DSC and GTI acquired baseline data of the 60-million-Btu/h host boiler with its existing low NO_x burner (shown in Table 3).

The 60-million-Btu/h commercial prototype burner was fabricated, installed, and shaken down at the host site. The burner/boiler successfully passed inspection by Factory Mutual. Shakedown of the installed commercial prototype burner revealed NO_x levels as low as 9.2 vppm. However, CO emissions were very high (~900 vppm). It was believed at the time that the high CO levels were a result of poor mixing in the secondary zone.

Table 3. Baseline Data for 60-million-Btu/h Host Boiler

Load, million Btu/h	24	26	38	40
FGR, %	36	16	16	58
O ₂ , %	3.1	2.6	2.2	1.7
NO _x , vppm	23.7	33.9	47.9	24.3
CO, vppm	152	182	175	169

Two modifications to the secondary air tip design were implemented for enhanced mixing and additional CO burnout. Preliminary tests during September 1999 confirmed stable operation from 12 to 60 million Btu/h, but NO_x and CO stack emissions were still above target. It was determined that the primary air to fuel ratio was too high, and further work was needed to characterize the stoichiometry across the load range. Several concepts were discussed which would allow additional control of the primary to secondary air distribution. A register to control the amount of primary air was designed and fabricated, and the primary nozzle design was modified to obtain more uniform combustion. In addition, to improve CO burnout, a new secondary air tip was fabricated based on a design used successfully in previous FIR burner installations. However, none of these steps were able to reduce stack CO levels sufficiently, as stack emissions were still above target (13.6 vppm NO_x and >1000 vppm CO). Sampling of the fuel-air mixture at four locations in the primary distribution plenum and analysis by gas chromatography (O₂, N₂, and CH₄) showed good uniformity, ruling out poor fuel distribution as a source of high CO levels.

Extensive sampling was then performed to determine the origin of high CO, as shown in Figure 6. Sampling at three locations about 14" downstream of the secondary air tip (pts 1-3) showed much lower CO levels (70-380 vppm) than the stack. A sampling probe was inserted from the back of the boiler 6 feet into the combustion chamber (pt 4), which showed very low CO levels (4-6 vppm). Further sampling at locations just upstream of the economizer (pt 24) and at the transition to the economizer still revealed CO levels ranging from several hundred to several thousand vppm. Table 4 shows data from these four sampling locations. Based on these initial findings, it was concluded that a short-circuiting of combustion gases from the substoichiometric primary zone may be occurring though the boiler wall separating the combustion chamber from the convective pass. Additional sampling ports were opened into the boiler to investigate this possibility. Sampling was performed inside the convective pass (pts 5-11) and in the transition duct from the convective pass to the economizer inlet (pts 12-23).

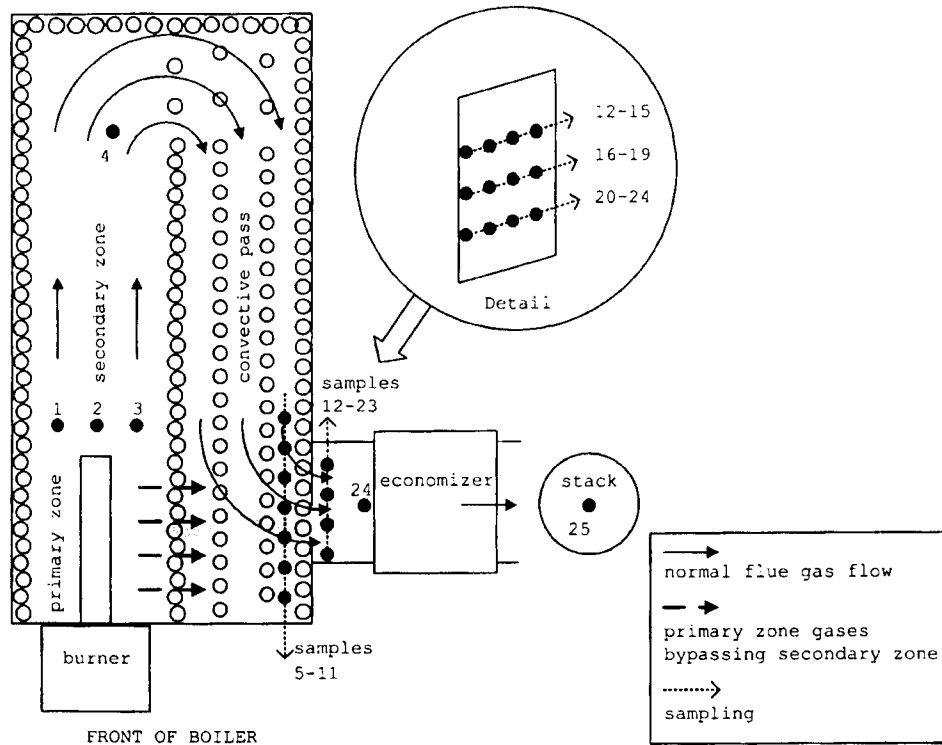


Figure 6. Sampling to Determine Source of High Stack CO Levels

Table 4. Emissions Mapping in 60-million-Btu/h Boiler

Load, million Btu/h	31	34	31	34
Sampling Location (point #)	Secondary zone (2)	Furnace exit (4)	Economizer inlet (24)	Stack (25)
O ₂ , %	5.8	4.3	4.2	4.1
NO _x , vppm	8.2	14.3	11.6	12.5
CO, vppm	177	4	1794	2005

These tests confirmed that combustion gases from the first stage of the FIR burner were traveling through gaps between the tangent tubes of the convective wall at a location shown by the shaded areas in Figure 6. Visual observations later confirmed the presence of gaps up to 1/8 inch, which could explain higher-than-expected NO_x and CO emissions. The higher NO_x could be caused by aspiration of flue gases containing excess O₂ into the root of the primary combustion zone, where the pressure is likely lower than in the convective pass, and the higher

CO is definitely caused by the bypassing flow of the fuel rich primary zone combustion products into the convective pass.

The project team contacted the boiler manufacturer and evaluated approaches to seal the boiler furnace/convective pass wall. A preferred method was selected and implemented in December 1999, which consisted of "stitch-welding" 1/4-inch steel rods between the tangent tubes and filling the remaining gaps with trowelable refractory. This measure reduced stack CO by about 90%, but CO levels were still in the range of 300-500 vppm. The site permit requires 400 vppm CO.

The boiler was then taken out of service for regular maintenance, and was brought into continuous automatic service in March 2000, being used mainly for load-following duty while another boiler was shut down for scheduled maintenance.

Further modifications were selected and implemented as described under Task III-9 below.

Task III-6. Data Reduction and Analysis

The experimental data collected during Task 5 were reduced and analyzed, and the results are described above.

Task III-7. Business Plan

As of December 31, 2001, a licensing agreement is under negotiation with Coen Company, Inc., a major U.S. manufacturer of boiler burners. In addition, a subcontract is also under review with Coen for engineering and testing services for the 5-vppm FIR burner development tasks. Coen is also planning to commit substantial cost sharing of their activities.

As a part of their contribution to the project, Coen will address all functional activities (e.g., technical, marketing, engineering, manufacturing, distribution, sales, finance, human resources and legal) necessary to support FIR burner commercialization. Coen is the leading U.S. manufacturer of burners for package watertube and firetube boilers, and has stated a willingness to aggressively market the FIR burner in both 9-vppm and 5-vppm configurations.

Task III-8. Project Management and Reporting

GTI has submitted quarterly project status reports, Milestone Logs, and Milestone Status Reports according to DOE reporting requirements. In addition, an annual IEA Implementing Agreement "Energy Conservation and Emissions Reduction in Combustion" report was prepared and submitted.

Task III-9. Burner Field Testing and Boiler Modifications

Following the diagnosis of the source of high stack CO in field testing of the 60-million-Btu/h boiler at the southern California brewery, the project team made a decision to implement a

permanent solution by reconfiguring the burner to a design with lean primary stage combustion (fuel-air staging).

The intended modifications were tested on the 6-million-Btu/h flexible burner at the GTI laboratory, which confirmed the ability to minimize the impact of boiler wall leakage while maintaining low NO_x and excellent fuel burnout.

A detailed design package for the 60-million-Btu/h prototype burner modifications was prepared, fabrication was completed in June 2000, and testing at the brewery resumed in July 2000. The modified burner eliminated high stack CO and improved NO_x emissions in the range of 17 to 55 million Btu/h, as shown in Table 5.

Table 5. 60-million-Btu/h Prototype FIR Burner Performance in July 2000

Load, million Btu/h	15	31	41	51	55
Load, %	25	52	68	85	93
O ₂ , %	4.6	4.6	4.5	5.0	5.1
NO _x , vppm	7.4	7.0	8.6	8.5	9.5
CO, vppm	60	5.4	6.5	3.3	3.4

Task III-10. Burner Optimization and Extended Field Testing

Additional minor modifications were designed to bring the burner up to full-load capability, and these were implemented in October 2000. Performance targets for NO_x and CO emissions were met at 18 to 60 million Btu/h, although CO emissions at lowest load (15 million Btu/h) continued to be above the 30 vppm target, as indicated by the data in Table 6.

Table 6. 60-million-Btu/h Prototype FIR Burner Performance in October 2000

Load, million Btu/h	15	31	41	51	60
Load, %	25	52	68	85	100
O ₂ , %	4.6	4.6	4.5	5.0	5.7
NO _x , vppm	7.4	7.0	8.6	8.5	7.7
CO, vppm	60	5.4	6.5	3.3	2.3

This performance represents a 65% NO_x reduction and a 96% CO reduction compared to baseline. In addition to meeting emissions targets, the use of the FIR burner increased boiler efficiency because of improvements in boiler operation related to the FIR burner installation. After comparing stack temperatures and FGR fan power demand, and accounting for the slightly elevated excess air requirement for optimal FIR operation, the net energy efficiency improvement was about 1.0%.

The burner and control system were then characterized for routine operation in automatic regime on this boiler. The host site scheduled a series of routine boiler outages for their three other boilers during early 2000, and the commercial prototype burner was made available to the host facility as needed during that period. The Boiler No. 3/FIR burner was carrying load swings during the Boiler Nos. 1, 2, and 4 outages with stable operation.

In addition to improved emissions, boiler efficiency compared to baseline operation was increased 1.5 percentage points with the FIR burner. The burner has been operating in automatic regime since July 2000, providing steam for plant operations. The host site operator was pleased with the FIR burner performance and decided to purchase the burner. A permit was submitted to the South Coast Air Quality Management District for burner operation. A Relative Accuracy Test Audit (RATA) compliance test was performed on the boiler, and the resulting deviation in measurement was within the required 7.5%, which permits testing to be conducted on an annual basis.

Task III-11. Development of a 5-vppm-NO_x Burner for Watertube Boilers

This work was directed towards development of an FIR burner version capable of 5-vppm NO_x performance on a watertube boiler. The 6-million-Btu/h laboratory (flexible test) burner was modified to accommodate distributed heat release by controlled jet penetration and intermediate air injection into selected regions of the primary zone. Parametric testing of the modified burner to validate the beneficial effects of advanced design features was conducted. Operating conditions were selected to simulate field operation as closely as possible. Modeling was applied to assist in the formation of burner design details. The experimental data was evaluated with model predictions based on combustion chemistry kinetics and fluid dynamics.

Under this Task, 426 tests were performed with 35 different burner configurations (Table 7). In these tests, NO_x levels as low as 3 vppm together with CO levels less than 10 vppm were achieved under some conditions. Particular attention was paid to the relationship between achievable NO_x levels, light-off ability, and flame stability over the entire load range. A set of design principles were established for design of an advanced ultra-low-NO_x burner for watertube boilers, assuming continuing progress in achieving the goal of 5 vppm NO_x across the entire operating range.

From analysis of these data, five major design elements were selected for incorporation into the 5-vppm burner design:

- Uniform primary nozzle diameter (nozzle velocity) and uniform distribution of primary nozzles relative to boiler wall;
- Maximum nozzle velocity obtainable from available combustion air pressure;
- Optimization of staging "window", i.e., primary close to fuel-lean limit with secondary fuel-rich as necessary to regain normal fuel efficiency;
- Maximum mixedness of secondary fuel-air mixture via turbulence-promoting secondary tip design;

- Optimal injection angle of secondary mixture to mix properly with first-stage combustion products.

Table 7. Summary of Burner Versions Investigated for 5-vppm NOx Performance

#	Version	Description / changes
1	A	Baseline design with alloy recirculation sleeve
2	B	Mixed larger- and smaller-ID primary nozzles
3	C	Smaller number of larger-ID primary nozzles
4	D	Version C + intermediate air injection
5	E	Changed intermediate air injection location
6	F	Changed intermediate air injection location
7	G	Version C + intermediate fuel injection
8	H	Changed intermediate fuel injection location
9	J	Version A + secondary fuel injection w/ distributor design J
10	K	Version A + secondary premixed fuel-air injection w/ distributor design K
11	L	Larger secondary nozzles
12	M	Primary nozzle arrangement M + secondary premix w/ distributor design L
13	N	Version A + intermediate fuel + secondary premix w/ distributor design N
14	O	Removed intermediate fuel injection
15	P	Smaller secondary nozzle ID
16	R	Changed secondary nozzle longitudinal angle
17	S	Changed secondary nozzle transverse angle
18	T	Smaller secondary nozzle ID
19	U	Alternating secondary nozzle transverse angle
20	V	Applied recirculation sleeve coating
21	W	Eductor-style secondary nozzles + no sleeve coating
22	Y	Water-cooled insert in primary zone
23	Z	Secondary tip as in version P
24	AA	Secondary tip as in version U
25	AB	Non-metallic recirculation sleeve
26	AC	Insulated secondary air tube
27	AD	Thinner secondary air tube insulation
28	AE	Different non-metallic recirculation sleeve
29	AG	Fully premixed secondary + no secondary air tube insulation
30	AI	Different non-metallic recirculation sleeve + new secondary tip design
31	TSA	Thermal staging design
32	TSB	Larger primary nozzle ID
33	TSC	Larger primary nozzle ID
34	TSD	Primary nozzle restrictor to change primary:secondary distribution
35	TSE	Smaller primary nozzle restrictor

This testing was also guided by information obtained from experience in the field, particularly with respect to the influence of boiler combustion chamber geometry on burner performance. Comparison of laboratory data with field test data strongly suggests that accurate prediction of burner performance in watertube boiler applications would require developmental testing on an actual boiler of similar geometry. For this reason, GTI proceeded to locate, procure, and install a 20-million-Btu/h watertube package boiler for continuing ultra-low-NO_x burner development.

The design of a 20-million-Btu/h advanced burner for performance validation on the watertube boiler was initiated, incorporating a number of features to allow flexibility for continuing development, such as movable and removable fittings, supports, etc. The design of the scaled-up burner was developed to include, in general, the following features guided by the results of boiler simulator testing:

- Combined version of staging
- Optimized fuel and air mixing in both stages
- Burner geometry which maximizes the uniformity of flame temperature and heat transfer to the boiler walls

Coen, with GTI support, will produce an engineering design package for a 20-million-Btu/h commercial prototype FIR burner, based on the results of Task 11. Following design review by the project team, any required changes will be made and Coen will fabricate the burner. The prototype burner will be installed on the new watertube test boiler at the GTI combustion laboratory and demonstrated to validate the projected performance. Coen will also optionally find an industrial host site for the 20-million-Btu/h burner, although it is not required if the demonstration at GTI is successful.

The results of the prototype demonstration will also be used to update CFD models of the burner and provide the basis for a CFD model of the boiler/burner system as required to support commercialization activities.

Finally, the project team also plans to design a 50-million-Btu/h commercial prototype burner which will be demonstrated at an industrial host site in future years.

Patents

No patent applications were applied for under this project.

Publications

The following papers based on this project have been published or presented:

- Pratapas, J., "Forced Internal Recirculation Burner," presented at NOx Control XIV, Council of Industrial Boiler Owners, San Diego, California, March 12, 2001.
- "21st Task Leaders Meeting of the International Energy Agency's Implementing Agreement on Energy Conservation and Emissions Reduction in Combustion," Presentation at the Ohtsu, Shiga, Japan, September 27, 1999.
- Rabovitser, J., D. Cygan, R. Knight T. Giaier, D. Cron, I. Chan, H. Mak, "Demonstration of Ultra-Low-NOx FIR Burners on Watertube and Firetube Boilers," presented at IndTech '99, American Boiler Manufacturers Association Technical Conference, Anaheim, California, September 22, 1999.
- Rabovitser, J., D.F. Cygan, and M.J. Khinkis, "FIR Burner Achieves Sub 10 vppm NOx Without FGR," in Proc. 1998 International Gas Research Conference, 763-69, November 9-11, 1998.
- "20th Task Leaders Meeting of the IEA Implementing Agreement Energy Conservation and Emissions Reduction in Combustion," Presentation at the Government Conference Centre, Ottawa, Canada, July 27, 1998.
- Giaier, T., D. Cron, D. F. Cygan, and J. Rabovitser. "FIR Low-NOx Burner," presented at the Council of Industrial Boiler Owners Annual Meeting, Corpus Christi, Texas, February 10, 1998.
- Giaier, T., et al., "20 MMBtu/h FIR Burner Test Results: High-Efficiency and Very Low-NOx With No FGR," presented at the AFRC 1997 International Symposium, Chicago, September 21-24, 1997.
- "19th Task Leaders Meeting of the IEA Implementing Agreement Energy Conservation and Emissions Reduction in Combustion," I. Rabovitser, D. F. Cygan, M. Roberts, H. Abbasi, T. Giaier and D. Cron. Presentation at the Palazzo dei Congressi, Capri, Italy, September 16, 1997.
- "18th Task Leaders Meeting of the IEA Implementing Agreement Energy Conservation and Emissions Reduction in Combustion," B. Soroka, I. Karp, M. Roberts, D. F. Cygan and F. Lisin. Presented at the School of Mechanical Engineering, Cranfield University, Cranfield, U.K., August 6-9, 1996.
- Roberts, M.J., M. J. Khinkis, D. F. Cygan, B. Sinn, and D. Scarpiello, "An Ultra-Low Emissions Forced Internal Recirculation Burner for Boilers and Process Heaters," *Preprints of the 1995 International Gas Research Conference*, 404-12, June 1995.

Technical Report
For
Joseph K. Rabovitser
Institute of Gas Technology
Prepared by
Prof. A. Fridman, and
Dr. S. Nester

Analytical and Numerical Studies of the Chemical Mechanisms of NO_x Formation in Premixed Natural Gas/Air Flames

University of Illinois at Chicago
January 14, 1999

Background

Nitrogen chemistry in combustion processes has been the subject of intensive studies for more than fifty years. This research is motivated by the impact of pollutants from the combustion in to the environment. Presently, explanations of how these pollutants are formed are summarized in the form of complex reaction mechanisms. NO_x formation in natural gas combustion is contributed due to three distinct paths of formation namely: Zeldovich mechanism, N_2O - intermediate mechanism and Prompt NO mechanism.

Normal levels of NO_2 emission in natural gas flames usually do not exceed 5% of the total NO_x amount. The NO_2 concentration can be explained by the fact that NO_2 exist only as transient species at flame temperatures. As a transient specie, they are easily distracted by reactions with hydrogen/oxygen atoms producing NO and OH/O_2 . Primary reaction of NO_2 formation is the reaction between NO and HO_2 radical, which is present typically in low-temperature flame regions.

Experimental studies have shown significant increase of NO_2 fractions in NO_x emissions from some combustion sources such as gas turbines, gas appliances and turbulent flames of natural gas. In turbulent flames, the NO_2/NO_x ratio increases with the increase in the Reynolds number of the flow. Finally, in situ measurements of NO_x concentrations in premixed and non-premixed flames have shown relatively large NO_2/NO_x ratios in the regions near the flame zone. Generally, to receive noticeable concentrations of NO_2 it is necessary to create special conditions. Usually those conditions are associated with rich mixtures and turbulent jet flames. In these situations, the increase in NO_2 production can be explained qualitatively by quenching occurring by rapid mixing of the hot and cold gas elements.

A Natural Gas Premixed Forced Internal Recirculation Burner (FIR) was designed to decrease NO_x production when burning natural gas at low excess air. The burner consists of two stages. In the primary stage, combustion of rich natural gas - air mixture occurs at temperatures of 800K. In the secondary stage, air directed through the primary combustion zone, provides final oxidation of the unburned hydrocarbons. This design permits the reduction of NO_x emission by lowering the overall combustion temperature. For the FIR burner NO_x emission, levels are lower then 10 vppm while preserving the low levels of CO and total hydrocarbon emissions. The measured NO_x emission consists of 60 to 80% of NO_2 . This differs significantly from NO. compositions in regular burners were NO_2 does not exceed 5% of total NO_x amount.

To explain the low temperature combustion in the first stage of the burner a detailed chemical mechanism was developed. According to this mechanism, the combustion proceeds through the degenerate chain branching mechanism. The main steps of the chain initiation are: slow methane oxidation presented by the elementary reaction: $\text{CH}_4 + \text{O}_2 \rightleftharpoons \text{CH}_3 + \text{HO}_2$;
reaction of molecular oxygen destruction: $\text{CH}_3 + \text{O}_2 \rightleftharpoons \text{CH}_3\text{OO}$;

and reactions of chain propagation: $\text{CH}_3\text{OO} + \text{CH}_4 \rightleftharpoons \text{CH}_3\text{OOH} + \text{CH}_3$; $\text{CH}_3\text{OOH} \rightarrow \text{CH}_3\text{O} + \text{OH}$.

For the explanation of low NO_x emission levels and anomalous NO_2/NO ratios in rich low-temperature flames a detailed chemical NO_x formation mechanism was developed. In rich premixed flames at the temperatures varying from 700 to 1000K, the predicted reaction path of the NO_x formation proceeds through the reactions between molecular nitrogen and CH_n radicals. Abnormally high NO_2 percentage was explained due to high HO_2 concentration in the flame. The comparison of numerical and experimental results is provided.

Introduction

Low- NO_x burners are one of the most extensively developing NO_x control technologies. Most of these devices reduce NO_x emissions typically in the range 30-50% at a moderate cost [1,21]. Main strategies of NO_x control include fuel-staging, air-staging in its different variants [3] as well as utilization of oxygen instead of air in Oxy-fuel burners. The main reason behind first two strategies is to reduce the temperature of air-fueled combustion and therefore minimize the thermal reactions paths leading to NO_x formation.

In FIR burner registered temperatures in the primary combustion zone were as low as 800K. In the low temperature regimes at 700-1000K the oxidation of hydrocarbons proceeds through a very complex chemical mechanism involving different propagation and chain branching reactions. Such phenomena as relatively slow oxidation times and negative temperature dependence of oxidation rates are well known in low temperature. Because of the negative temperature dependence of oxidation rates, cool flames require heat losses, while ignitions can take place in adiabatic conditions. That leads to many specific cool flames phenomena such as oscillatory cool flames, single-, two-, and multi stage ignitions. Those low temperature phenomena are the result of interactions between chemical kinetics and heat release. The oxidation chemistry in the cool flames historically was studied mostly for hydrocarbons beginning from C_2 and higher due to its importance in C.T. engines, and knock phenomena in S.I. engines. An extensive literature review can be found in [41 see also [5,6,7,8].

For a long time, it was believed that cool flames do not exist in methane until 1956 [9] when Vanpee published his first experimental results on the cool flames of methane in the rich methane-air mixture containing 67% of methane. The current observations show that cool flames of methane exist in the temperatures starting from 720K and are most stable at the temperature of 780 to 820K where the cool flame is most extensive. Methane-air cool flames exist under pressures starting from 50 cm Hg and higher, they can be non-luminous, pale blue, blue or bright yellow. Self-ignition times in these flames can be as high as 5-7sec. and characteristic combustion times are less than one second. Qualitatively ignition diagrams and flame phenomena of methane and of higher hydrocarbons are very similar. It is found, though, that the temperature of the maximum flame intensity for methane flame is higher than those for higher hydrocarbons. This temperature is 613K for n-hexane, 623K for n-pentane, 588K for n-butane, 583K for

propane 593K for ethane and 788K for methane. This notable difference in temperature between methane and other hydrocarbons shows that mechanism of methane combustion differs from those of higher hydrocarbons [10]. In spite, the fact that the experimental characteristics of methane cool flames are known, the chemistry of methane oxidation at those low temperatures still needs explanation. In the present paper, the description of chemical mechanism of this phenomenon is presented.

The formal initiation of current work was an attempt to explain quantitatively the low NO_x concentrations and extremely high NO_2 to NO ratios in the FIR burner. The NO_2 to NO_x ratios reaching nearly 100% were registered in C_3H_8 flames under gas turbines conditions [14, 15, 16]. The current empirical explanation of the phenomenon is that rapid mixing in turbulent flames promotes conversion of NO to NO_2 by generated during the mixing process HO_2 radicals [17, 18]. NO_2 emissions were compared for turbulent K2 and CH_4 jet diffusion flames. In all of the flames studied in this work [13] NO_2 to NO increases with decreasing NO concentration in the flame and with decreasing adiabatic flame temperature. The NO_2 to NO is higher for CH_4 fuel and the effect of methane is most pronounced when a flame blowout limit is approached. The maximum NO_2 to NO_x level (40 %) was reached in the methane flame. However, all known observations of this effect were made for high combustion temperatures about 2000K. No quantitative explanation of this effect is known for high temperature burners.

The description of nitrogen chemistry in methane-air flames is been thoroughly investigated during the last 5 decades, detailed description of those mechanisms can be found in [11, 6, 12]. All those mechanisms were developed for temperatures 1200K and up. The main mechanism of NO_x production in methane air flames is known to be Zeldovich mechanism, however, at the temperature levels of 800K, the mechanism is not productive [11]. The main mechanism for NO_x production at low temperatures is hypothesized to be so called Prompt NO mechanism, where nitrogen is dissociated through the reactions with C , CH , and CH_2 radicals [11]. To find the concentrations of C , CH , and CH_2 radicals a low-temperature methane oxidation mechanism was developed. This mechanism represents the first part of the theoretical study in the paper. The second part of the paper presents a detailed chemical mechanism of low temperature NO_x formation. The numerical modeling of NO_x emission levels was performed and compared with experimental results. Based on these results the high NO_2 to NO ratios are explained and are consistent with the experimental observations of the dependence between HO_2 and NO_2 concentrations [12].

THEORETICAL ANALYSIS

Modeling Tools

In this study, a full implementation of CHEMKIN software package was used. The CHEMKIN software package, developed by the Sandia National Laboratory [301], contains two major components: the Interpreter and a Gas-Phase Subroutine Library. The Interpreter is a FORTRAN program, which reads and converts user-supplied chemistry describing the combustion process into a vectorized binary output file. The output file forms a link data file needed for the Gas-Phase Subroutine Library. The Gas-Phase Subroutine Library consists of number of FORTRAN programs that solve different kinetic related problems. To calculate the time- dependent chemical kinetics of NO_x emission in premixed natural gas system a Senkin and Premix programs were utilized. These two programs are capable of calculating the Temperature and species concentrations in a steady state system by solving nonlinear ordinary differential equations. The reacting mixture is treated as a closed system with no mass crossing into or out of the boundary. The total mass of the mixture is constant represented by:

$$m = \sum_{k=1}^K m_k \quad (1)$$

$$\frac{dm}{dt} = 0 \quad (2)$$

m_k is the mass of the k th species and K is the total number of species. The individual species are produced or destroyed according to:

$$\frac{dm_k}{dt} = V \omega_k W_k \quad k = 1, \dots, K \quad (3)$$

t is time, (ω_k) is the molar production rate of the k th species by elementary reaction, W_k is the molecular weight of the k th species, and V is the volume of the system. In terms of the mass fraction equation 3 can be written as:

$$\frac{dY_k}{dt} = v \omega_k W_k \quad k = 1, \dots, K \quad (4)$$

$Y_k = m_k/m$ represents the mass fraction of the k th species and $v=V/m$ is the specific volume. The net chemical production rate of each species results from a competition between all the chemical reactions involving that species. Each reaction proceeds according to the law of mass action and the forward rate coefficients are in the modified Arrhenius form:

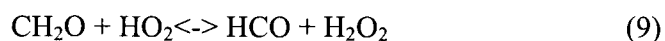
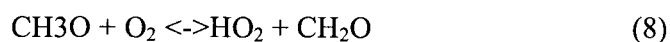
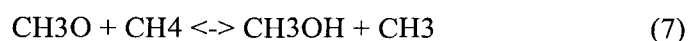
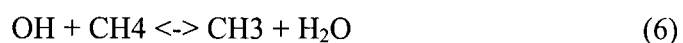
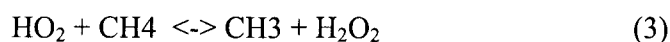
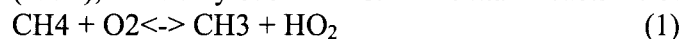
$$k_f = A T^P \exp\left(\frac{-E}{RT}\right) \quad (5)$$

where the activation energy represented by E , the temperature exponent by P and the pre-exponential constant A are parameters in the model formulation. The pre-exponential constants are the parameters considered for the sensitivity analysis.

For farther investigation of the data calculated by Senkin and Premix programs a Chemkin postprocessor programs such as Xsenkplot and Kinalc where used. Xsenkplot is capable of interactive computations and visualization of reacting flows. Whereas Kinalc is strictly sensitivity analysis program, it carries out three types of analysis: processing sensitivity analysis results, extracting information from the reaction rates and stoichiometry and provides kinetic information about the species.

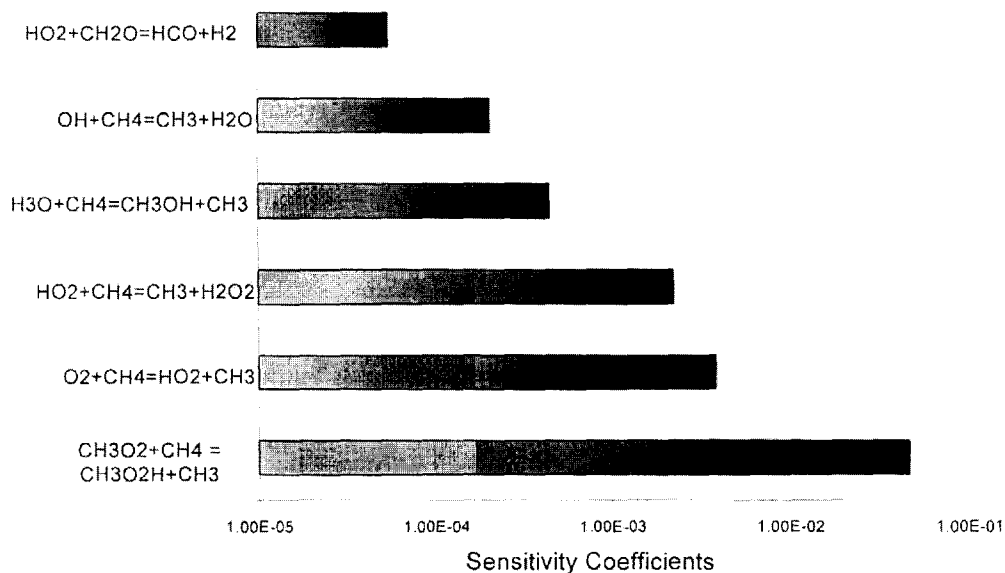
Low Temperature Combustion

Experimental results performed by IGT demonstrate a self-sustaining combustion occurring at the temperature levels of 800K. In order to explain combustion at such low temperature a set of reactions describing low temperature was introduced. This set of reactions forms a mechanism of methane oxidation describing methane/oxygen destruction with associated radical production. Existing kinetic methane oxidation mechanisms available in literature [19,11,21,22,23,24,25,26] were tried and found that they do not describe oxidation kinetics of methane for temperatures lower than 1500K. Our set of reactions is a degenerate chain branching oxidation mechanism similar to mechanisms of low temperature oxidation of C₂-C₃ hydrocarbons (such as propane, ethane, butane, etc...) presented by Kondratiev (1975), Glassman (1996), and Griffith (1995), and many other authors. The main reactions of that mechanism are:

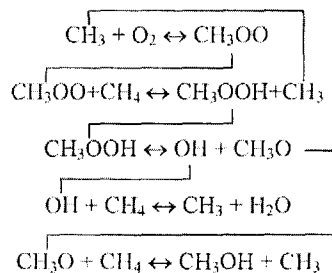


This reaction set (low-temperature combustion mechanism) describes production of short living CH₃ and OH radicals supporting combustion of methane. The mechanism also produces long living (at 800K) radicals such as HO₂, CH₃OOH and CH₃OO. The reaction: CH₃OO+CH₄ <-> CH₃OOH+CH₃, is the most important reaction in the overall process of methane dissociation into CH₃ radical. The sensitivity analysis performed for methane oxidation shown in Figure 1 shows the scale of importance for each of the participating reaction.

Figure 1



According to this mechanism, combustion at 800K proceeds not through direct dissociation of methane $\text{CH}_4 + \text{M} \leftrightarrow \text{CH}_3 + \text{H} + \text{M}$, but through the reactions of long living radicals and molecules such as HO_2 , CH_3OOH , and CH_3OO . The most important reaction in the overall process is the $\text{CH}_3\text{OO} + \text{CH}_4 \leftrightarrow \text{CH}_3\text{OOH} + \text{CH}_3$. The importance of the $\text{CH}_3\text{OO} + \text{CH}_4 \leftrightarrow \text{CH}_3\text{OOH} + \text{CH}_3$ reaction is evident due to the production of two important species CH_3 and CH_3OOH . CH_3OOH species are the primary source of two important radicals – OH and CH_3O through the branching reaction $\text{CH}_3\text{OOH} \leftrightarrow \text{CH}_3\text{O} + \text{OH}$, which decompose methane and oxygen. CH_3 radicals dissociate oxygen through the reaction $\text{CH}_3 + \text{O}_2 \leftrightarrow \text{CH}_3\text{OO}$ starting the chain propagation and branching of the low temperature mechanism:



The oxidation of methane can be explained through the role of large long living CH₃OO radicals and CH₃OOH molecules. Chemical reactions of those species have lower activation energies (comparing to reactions of high temperature methane oxidation), and are the primary agents for CH₄ destruction forming CH₃ radical. With the increases of temperature the equilibrium in the reaction CH₃ + O₂ <-> CH₃OO is shifted left resulting in destruction of large molecules. The rates of other reactions of active radicals with oxygen such as R + O₂ <-> olefin + HO₂ also increase. Those effects slow down the overall oxidation process. The slow down of oxidation process is known as negative temperature coefficient. The large CH₃OOH and CH₃OO Molecules dissociate at high temperatures. For example CH₃OO radical quickly decomposes into CH₃ and O₂ leading to the chain-terminating reaction CH₃OO <-> CH₃ + O₂. The reaction CH₃OO <-> CH₃ + O₂ stops further oxidation of methane making the low temperature mechanism unimportant at higher temperatures.

Detailed Chemical Combustion Mechanism:

The detailed combustion mechanism for kinetic modeling was composed from our low-temperature combustion mechanism and reactions presented in GRI-MECH 2.11 [12]. The full set contains 285 elementary chemical reactions. The rate constants for low temperature reactions were chosen based on the Chemical Kinetics database developed by National Institute of Standards and Technology (NIST) or obtained from literature [291]. All calculations were performed using Chemkin software package. The mechanism as used in Chemkin Interpreter is as follow:

REACTIONS CONSIDERED

($k = A T^b \exp(-E/RT)$)

	A	b	E
Low Temperature Reactions			
CH ₄ (+M)=CH ₃ +H(+M)	2.400E+16	.000	104500.00
HO ₂ +CH ₃ <=>O ₂ +CH ₄	1.000E+12	.000	.00
CH ₃ +O ₂ =>CH ₃ O ₂	3.000E+11	.000	.00
CH ₃ O ₂ +CH ₄ =>CH ₃ O ₂ H+CH ₃	1.800E+11	.000	18500.00
CH ₃ O ₂ H=>CH ₃ O+OH	3.700E+39	.000	42300.00
CH ₃ O+CH ₄ =>CH ₃ OH+CH ₃	3.730E+11	.000	8843.00
CH ₃ OH+O ₂ =>CH ₂ OH+HO ₂	3.047E+13	.000	44911.00
CH ₃ +CH ₃ OH<=>CH ₂ OH+CH ₄	3.000E+07	1.500	9940.00
O ₂ +CH ₂ O<=>HO ₂ +HCO	1.000E+14		.000
40000.00			
2HO ₂ <=>O ₂ +H ₂ O ₂	4.200E+14	.000	12000.00
HO ₂ +CH ₂ <=>OH+CH ₂ O	2.000E+13	.000	.00
HO ₂ +CH ₃ <=>OH+CH ₃ O	1.500E+11	.000	.00
HO ₂ +CH ₂ O<=>HCO+H ₂ O ₂	1.000E+12	.000	8000.00
CH ₃ +O ₂ <=>O+CH ₃ O	2.675E+13	.000	28800.00
CH ₃ +O ₂ <=>OH+CH ₂ O	3.600E+10	.000	8940.00
CH ₃ +H ₂ O ₂ <=>HO ₂ +CH ₄	2.450E+04	2.470	5180.00

CH2OH+O2<=>HO2+CH2O	1.800E+13	.000	900.00
CH3O+O2<=>HO2+CH2O	4.280E-13	7.600	-3530.00
CH3O2=>CH3+O2	1.250E+11	.000	33248.00
CH3O2+CO=>CH3O+CO2	1.000E+14	.000	20000.00
CH3O2+CH3OH=CH3O2H+CH2OH	1.800E+12	.000	13700.00
CH3O2+CH2(S)=CH2O+CH3O	1.800E+13	.000	.00
CH3O2+C2H2=CH3O2H+C2H	5.600E+11	.000	24500.00
CH3O2+C2H4=CH3O2H+C2H3	3.900E+12	.000	24500.00
CH3O2+C2H6=CH3O2H+C2H5	2.900E+11	.000	14900.00

Reactions with O radical

2O+M<=>O2+M	1.200E+17	-1.000	.00
O+H+M<=>OH+M	5.000E+17	-1.000	.00
O+CH4<=>OH+CH3	1.020E+09	1.500	8600.00
O+CH3<=>H+CH2O		8.430E+13	.000
.00			
O+CH2<=>H+HCO	8.000E+13	.000	.00
1.500E+13 .000 .00			
O+CH2(S)<=>H+HCO	1.500E+13	.000	.00
O+C2H<=>CH+CO	5.000E+13	.000	.00
O+C2H2<=>H+HCCO	1.020E+07	2.000	1900.00
O+C2H2<=>OH+C2H	4.600E+19	-1.410	28950.00
O+C2H2<=>CO+CH2	1.020E+07	2.000	1900.00
O+C2H3<=>H+CH2CO	3.000E+13	.000	.00
O+C2H4<=>CH3+HCO	1.920E+07	1.830	220.00
O+C2H5<=>CH3+CH2O	1.320E+14	.000	.00
O+C2H6<=>OH+C2H5	8.980E+07	1.920	5690.00
O+H2<=>H+OH	5.000E+04	2.670	6290.00
O+HO2<=>OH+O2	2.000E+13	.600	.00
O+H2O2<=>OH+HO2	9.630E+06	2.000	4000.00
O+HCO<=>OH+CO	3.000E+13	.000	.00
O+HCO<=>H+CO2	3.000E+13	.000	.00
O+CH2O<=>OH+HCO	3.900E+13	.000	3540.00
O+CH2OH<=>OH+CH2O	1.000E+13	.000	.00
O+CH3O<=>OH+CH2O	1.000E+13	.000	.00
O+CH3OH<=>OH+CH2OH	3.880E+05	2.500	3100.00
O+CH3OH<=>OH+CH3O	1.300E+05	2.500	5000.00
O+HCCO<=>H+2CO	1.000E+14	.000	.00
O+CH2CO<=>OH+HCCO	1.000E+13	.000	8000.00
O+CH2CO<=>CH2+CO2	1.750E+12	.000	1350.00
O+CO+M<=>CO2+M	6.020E+14	.000	3000.00

Reactions with H radical

H+O2+M<=>HO2+M	2.800E+16	-.860	.00
H+O2=>HO2	4.515E+13	.000	.00

H+2O2 \rightleftharpoons HO ₂ +O ₂	3.000E+20	-1.720	.00			
H+O2+H2O \rightleftharpoons HO ₂ +H2O	9.380E+18	-.760	.00			
H+O2+N ₂ \rightleftharpoons HO ₂ +N ₂	3.750E+20	-1.720	.00			
H+O2+AR \rightleftharpoons HO ₂ +AR	7.000E+17	-.800	.00			
H+O2 \rightleftharpoons O+OH	8.300E+13	.000	14413.00			
2H+M \rightleftharpoons H ₂ +M	1.000E+16	-1.000	.00			
2H+H ₂ \rightleftharpoons 2H ₂	9.000E+16	-.600	.00			
2H+H2O \rightleftharpoons H ₂ +H2O	6.000E+19	-1.250	.00			
2H+CO ₂ \rightleftharpoons H ₂ +CO ₂	5.500E+20	-2.000	.00			
H+OH+M \rightleftharpoons H2O+M	2.200E+22	-2.000	.00			
H+HO ₂ \rightleftharpoons O+H2O	3.970E+12	.000	671.00			
H+HO ₂ \rightleftharpoons O2+H ₂	2.800E+13	.000	1820.00			
H+HO ₂ \rightleftharpoons 2OH	1.340E+14	.000	635.00			
H+H2O ₂ \rightleftharpoons HO ₂ +H ₂	1.210E+07	2.000	5200.00			
H+H2O ₂ \rightleftharpoons OH+H2O	1.000E+13	.000	3600.00			
H+CH \rightleftharpoons C+H ₂	1.100E+14	.000	.00			
H+CH ₂ (+M) \rightleftharpoons CH3(+M)	2.500E+16	-.800	.00			
H+CH ₂ (S) \rightleftharpoons CH+H ₂	3.000E+13	.000	.00			
H+CH4 \rightleftharpoons CH ₃ +H ₂	6.600E+08	1.620	10840.00			
H+HCO(+M) \rightleftharpoons CH2O(+M)	1.090E+12	.480	-260.00			
H+HCO \rightleftharpoons H ₂ +CO	7.340E+13	.000	.00			
H+CH2O(+M) \rightleftharpoons CH2OH(+M)	5.400E+11	.454	3600.00			
H+CH2O(+M) \rightleftharpoons CH ₃ O(+M)	5.400E+11	.454	2600.00			
H+CH2O \rightleftharpoons HCO+H ₂	2.300E+10	1.050	5180.00			
H+CH2OH(+M) \rightleftharpoons CH ₃ OH(+M)	1.800E+13	.000	.00			
H+CH2OH \rightleftharpoons H ₂ +CH2O	2.000E+13	.000	.00			
H+CH2OH \rightleftharpoons OH+CH ₃	1.200E+13	.000	.00			
H+CH2OH \rightleftharpoons CH ₂ (S)+H2O	6.000E+12	.000	.00			
H+CH ₃ O(+M) \rightleftharpoons CH ₃ OH(+M)	5.000E+13	.000	.00			
H+CH ₃ O \rightleftharpoons H+CH2OH	3.400E+06	1.600	.00			
H+CH ₃ O \rightleftharpoons H ₂ +CH2O	2.000E+13	.600	.00			
H+CH ₃ O \rightleftharpoons OH+CH ₃	3.200E+13	.000	.00			
H+CH ₃ O \rightleftharpoons CH ₂ (S)+H2O	1.600E+13	.000	.00			
H+CH ₃ OH \rightleftharpoons CH2OH+H ₂	6.000E+08	.000	.00			
H+CH ₃ OH \rightleftharpoons CH ₃ O+H ₂	4.200E+06	2.100	4870.00			
H+C ₂ H(+M) \rightleftharpoons C ₂ H ₂ (+M)	1.000E+17	-1.000	.00			
H+C ₂ H ₂ (+M) \rightleftharpoons C ₂ H ₃ (+M)	5.600E+12	.000	2400.00			
H+C ₂ H ₃ (+M) \rightleftharpoons C ₂ H ₄ (+M)	61.080E+12	.270	280.00			
H+C ₂ H ₃ \rightleftharpoons H ₂ +C ₂ H ₂	3.000E+13	.000	.00			
H+C ₂ H ₄ (+M) \rightleftharpoons C ₂ H ₅ (+M)	1.080E+12		1820.00			
H+C ₂ H ₄ \rightleftharpoons C ₂ H ₃ +H ₂	1.325E+06	2.530	12240.00			
H+C ₂ H ₅ (+M) \rightleftharpoons C ₂ H ₆ (+M)	5.210E+17	-.990	1580.00			
H+C ₂ H ₅ \rightleftharpoons H ₂ +C ₂ H ₄	2.000E+12	.000	.00			
1.150E+08	1.900	7530.00	H+HCCO \rightleftharpoons CH ₂ (S)+CO	1.000E+14		
.000	.00		H+CH ₂ CO \rightleftharpoons HCCO+H ₂	5.000E+13	.000	8000.00

H+CH ₂ CO<=>CH ₃ +CO	1.130E+13	.000	3428.00
H+HCCOH<=>H+CH ₂ CO	1.000E+13	.000	.00

Reactions with OH radicals

OH+H ₂ <=>H+H ₂ O	4.500E+09	.000	.00
2OH(+M)<=>H ₂ O ₂ (+M)	7.400E+13	-.370	.00
2OH<=>O+H ₂ O	3.570E+04	2.400	-2110.00
OH+HO ₂ <=>O ₂ +H ₂ O	2.900E+13	.000	-500.00
OH+H ₂ O ₂ <=>HO ₂ +H ₂ O	1.750E+12	.000	320.00
OH+H ₂ O ₂ <=>HO ₂ +H ₂ O	5.800E+14		.000
9560.00			
OH+C<=>H+CO	5.000E+13	.000	.00
OH+CH<=>H+HCO	3.000E+13	.000	.00
OH+CH ₂ <=>H+CH ₂ O	2.000E+13	.000	.00
OH+CH ₂ <=>CH+H ₂ O	1.130E+07	2.000	3000.00
OH+CH ₂ (S)<=>H+CH ₂ O	3.000E+13	.000	.00
OH+CH ₃ (+M)<=>CH ₃ OH(+M)	6.300E+13	.000	.00
OH+CH ₃ <=>CH ₂ +H ₂ O	5.600E+07	1.600	5420.00
OH+CH ₃ <=>CH ₂ (S)+H ₂ O	2.501E+13	.000	.00
OH+CH ₄ <=>CH ₃ +H ₂ O	1.000E+08	1.600	3120.00
OH+HCO<=>H ₂ O+Co	5.000E+13	.000	.00
OH+CH ₂ O<=>HCO+H ₂ O	3.430E+09	1.180	-447.00
OH+CH ₂ OH<=>H ₂ O+CH ₂ O	5.000E+12	.000	.00
OH+CH ₃ O<=>H ₂ O+CH ₂ O	5.000E+12	.000	.00
OH+CH ₃ OH<=>CH ₂ OH+H ₂ O	1.440E+06	2.000	-840.00
OH+CH ₃ OH<=>CH ₃ O+H ₂ O	6.300E+06	2.000	1500.00
OH+C ₂ H<=>H+HCCO	2.000E+13	.000	.00
OH+C ₂ H ₂ <=>H+CH ₂ CO	2.180E-04	4.500	-1000.00
OH+C ₂ H ₂ <=>H+HCCOH	5.040E+05	2.300	13500.00
OH+C ₂ H ₂ <=>C ₂ H+H ₂ O	3.370E+07	2.000	14000.00
OH+C ₂ H ₂ <=>CH ₃ +C(D	4.830E-04	4.000	-2000.00
OH+C ₂ H ₃ <=>H ₂ O+C ₂ H ₂	5.000E+12	.000	.00
OH+C ₂ H ₄ <=>C ₂ H ₃ +H ₂ O	3.600E+06	2.600	2500.00
OH+C ₂ H ₆ <=>C ₂ H ₅ +H ₂ O	3.540E+06	2.120	870.00
OH+CH ₂ CO<=>HCCO+H ₂ O	7.500E+12	.000	2000.00
OH+CO=>H+CO ₂	8.127E+10	.000	.00

Reactions with C radicals

C+O ₂ <=>O+CO	5.800E+13	.000	576.00
C+CH ₂ <=>H+C ₂ H	5.000E+13	.000	.00
C+CH ₃ <=>H+C ₂ H ₂	5.000E+13	.000	.00

Reactions with CH radicals

CH+O2<=>O+HCO	1.000E+12	.000	.00
CH+O2<=>CO2+H	1.660E+13	.000	.00
CH+H2O<=>H+CH2O	1.713E+13	.000	-755.00
CH+CH2<=>H+C2H2	4.000E+13	.000	.00
CH+CH3<=>H+C2H3	3.000E+13	.000	.00
CH+CH4<=>H+C2H4	5.000E+13	.000	.00
CH+CO(+M)<=>HCCO(+M)	3.400E+12	.000	690.00
CH+CO2<=>HCO+CO	9.460E+13	.000	-515.00
CH+CH2O<=>H+CH2CO	5.000E+13	.000	.00
CH+HCCO<=>CO+C2H2			

Reactions with CH2 radicals

CH2+O2<=>OH+HCO	4.300E+10	.000	-500.00
CH2+H2=>H+CH3	1.110E+04	2.600	4980.00
CH2+CH3<=>H+C2H4	3.000E+13	.000	.00
CH2+CO(+M)<=>CH2CO(+M)	8.100E+11	.500	4510.00
CH2+HCCO<=>C2H3+CO	3.000E+13	.000	.00
CH2+O<=>CH+OH	5.000E+13	.000	.00
CH2+H<=>CH+H2	1.000E+18	-1.600	.00
CH2(S)<=>CH2	1.000E+13	.000	.00

CH2(S)+N2<=>CH2+N2	1.500E+13	.000	600.00
CH2(S)+O2<=>H+OH+CO	2.800E+13	.000	.00
CH2(S)+O2<=>CO+H2O	1.200E+13	.000	.00
CH2(S)+H2<=>CH3+H	7.000E+13	.000	.00
CH2(S)+H2O(+M)<=>CH3OH(+M)	2.000E+13	.000	.00
CH2(S)+H2O<=>CH2+H2O	3.000E+13	.000	.00
CH2(S)+CH3<=>H+C2H4	1.200E+13	.000	-570.00
CH2(S)+CH4<=>2CH3	4.000E+13	.000	.00
CH2(S)+CO<=>CH2+CO	9.000E+12	.000	.00
CH2(S)+CO2<=>CH2+CO2	7.000E+12	.000	.00
CH2(S)+CO2<=>CO+CH2O	1.400E+13	.000	.00
CH2(S)+C2H6<=>CH3+C2HS	4.000E+13	.000	-550.00

Reactions with CH3 radicals

2CH3<=>H+C2H5	4.990E+12	.100	10600.00
CH3+CH2O<=>HCO+CH4	3.320E+03	2.810	5860.00
CH3+C2H4<=>C2H3+CH4	2.270E+05	2.000	9200.00
CH3+C2H6<=>C2H5+CH4	6.140E+06	1.740	10450.00
HCO+H2O<=>H+CO+H2O	2.244E+18	-1.000	17000.00
HCO+M<=>H+CO+M	9.993E+13	.000	22000.00
HCO+O2<=>HO2+CO	3.311E+13	.000	7000.00
HCO+O2<=>HO2+CO	7.600E+12	.000	400.00

$\text{C}_2\text{H} + \text{O}_2 \rightleftharpoons \text{HCO} + \text{CO}$	5.000E+13	.000	1500.00
$\text{C}_2\text{H} + \text{H}_2 \rightleftharpoons \text{H} + \text{C}_2\text{H}_2$	4.070E+05	2.400	200.00
$\text{C}_2\text{H}_3 + \text{O}_2 \rightleftharpoons \text{HCO} + \text{CH}_2\text{O}$	3.980E+12	.000	-240.00
$\text{C}_2\text{H}_4(+\text{M}) \rightleftharpoons \text{H}_2 + \text{C}_2\text{H}_2(+\text{M})$	8.000E+12	.440	88770.00
$\text{C}_2\text{H}_5 + \text{O}_2 \rightleftharpoons \text{HO}_2 + \text{C}_2\text{H}_4$	8.400E+11	.000	3875.00
$\text{HCCO} + \text{O}_2 \rightleftharpoons \text{OH} + 2\text{CO}$	1.600E+12	.000	854.00
$2\text{HCCO} \rightleftharpoons 2\text{CO} + \text{C}_2\text{H}_2$	1.000E+13	.000	.00
$\text{CO} + \text{O}_2 \rightleftharpoons \text{O} + \text{CO}_2$	2.500E+12	.000	47800.00
$\text{CO} + \text{HO}_2 \rightleftharpoons \text{CO}_2 + \text{OH}$	3.498E+13	.000	8197.00
$\text{CO}(+\text{M}) + \text{H}_2 \rightleftharpoons \text{CH}_2\text{O}(+\text{M})$	4.300E+07	1.500	
79600.00			

Nitrogen Chemistry

Zeldovich Mechanism

$\text{N} + \text{NO} \rightleftharpoons \text{N}_2 + \text{O}$	3.500E+13	.000	330.00
$\text{N} + \text{O}_2 \rightleftharpoons \text{NO} + \text{O}$	2.650E+12	.000	6400.00
$\text{N} + \text{OH} \rightleftharpoons \text{NO} + \text{H}$	3.800E+14	.000	0.00

N₂O-intermediate mechanism

$\text{N}_2\text{O}(+\text{M}) \rightleftharpoons \text{N}_2 + \text{O}(+\text{M})$	1.300E+11	.000	59620.00
$\text{N}_2\text{O} + \text{O} \rightleftharpoons \text{N}_2 + \text{O}_2$	1.400E+12	.000	10810.00
$\text{N}_2\text{O} + \text{O} \rightleftharpoons 2\text{NO}$	2.900E+13	.000	23150.00
$\text{N}_2\text{O} + \text{H} \rightleftharpoons \text{N}_2 + \text{OH}$	4.400E+14	.000	18880.00
$\text{N}_2\text{O} + \text{OH} \rightleftharpoons \text{N}_2 + \text{HO}_2$	2.000E+12	.000	21060.00

Prompt NO

$\text{C} + \text{N}_2 \rightleftharpoons \text{CN} + \text{N}$	6.300E+13	.000	46020.00
$\text{CH} + \text{N}_2 \rightleftharpoons \text{HCN} + \text{N}$	2.000E+11	.000	13600.00
$\text{CH}_2 + \text{N}_2 \rightleftharpoons \text{HCN} + \text{NH}$	1.000E+13	.000	74000.00
$\text{CH}_2(\text{S}) + \text{N}_2 \rightleftharpoons \text{NH} + \text{HCN}$	1.000E+11	.000	65000.00

Reactions of NH

$\text{NH} + \text{O} \rightleftharpoons \text{NO} + \text{H}$	5.000E+13	.000	.00
$\text{NH} + \text{H} \rightleftharpoons \text{N} + \text{H}_2$	1.000E+14	.000	.00
$\text{NH} + \text{OH} \rightleftharpoons \text{HNO} + \text{H}$	2.000E+13	.000	.00
$\text{NH} + \text{OH} \rightleftharpoons \text{N} + \text{H}_2\text{O}$	2.000E+09	1.200	.00
$\text{NH} + \text{O}_2 \rightleftharpoons \text{HNO} + \text{O}$	4.610E+05	2.000	6500.00
$\text{NH} + \text{O}_2 \rightleftharpoons \text{NO} + \text{OH}$	1.280E+06	1.500	100.00

$\text{NH} + \text{N} \rightleftharpoons \text{N}_2 + \text{H}$	1.500E+13	.000	.00
$\text{NH} + \text{H}_2\text{O} \rightleftharpoons \text{HNO} + \text{H}_2$	2.000E+13	.000	13850.00
$\text{NH} + \text{NO} \rightleftharpoons \text{N}_2 + \text{OH}$	2.160E+13	-.230	.00
$\text{NH} + \text{NO} \rightleftharpoons \text{N}_2\text{O} + \text{H}$	4.160E+14	-.450	.00
$\text{NH} + \text{CH} \rightleftharpoons \text{HCN} + \text{H}$	5.000E+13	.000	.00

Reactions of NH_2

$\text{NH}_2 + \text{O} \rightleftharpoons \text{OH} + \text{NH}$	7.000E+12	.000	.00
$\text{NH}_2 + \text{O} \rightleftharpoons \text{H} + \text{HNO}$	4.600E+13	.000	.00
$\text{NH}_2 + \text{H} \rightleftharpoons \text{NH} + \text{H}_2$	4.000E+13	.000	3650.00
$\text{NH}_2 + \text{OH} \rightleftharpoons \text{NH} + \text{H}_2\text{O}$	9.000E+07	1.500	-460.00
$\text{NH}_2 + \text{CH} \rightleftharpoons \text{HCN} + \text{H} + \text{H}$	3.000E+13	.000	.00

Reactions of NNH

$\text{NNH} \rightleftharpoons \text{N}_2 + \text{H}$	3.300E+08	.000	.00
$\text{NNH} + \text{M} \rightleftharpoons \text{N}_2 + \text{H} + \text{M}$	1.300E+14	-.110	4980.00
$\text{NNH} + \text{O}_2 \rightleftharpoons \text{HO}_2 + \text{N}_2$	5.000E+12	.000	.00
$\text{NNH} + \text{O} \rightleftharpoons \text{OH} + \text{N}_2$	2.500E+13	.000	.00
$\text{NNH} + \text{O} \rightleftharpoons \text{NH} + \text{NO}$	7.000E+13	.000	.00
$\text{NNH} + \text{H} \rightleftharpoons \text{H}_2 + \text{N}_2$	5.000E+13	.000	.00
$\text{NNH} + \text{OH} \rightleftharpoons \text{H}_2\text{O} + \text{N}_2$	2.000E+13	.000	.00
$\text{NNH} + \text{CH}_3 \rightleftharpoons \text{CH}_4 + \text{N}_2$	2.500E+13	.000	.00

Reactions of HNO

$\text{H} + \text{NO} + \text{M} \rightleftharpoons \text{HNO} + \text{M}$	8.950E+19	-1.320	740.00
$\text{HNO} + \text{O} \rightleftharpoons \text{NO} + \text{OH}$	2.500E+13	.000	.00
$\text{HNO} + \text{H} \rightleftharpoons \text{H}_2 + \text{NO}$	4.500E+11	.720	660.00
$\text{HNO} + \text{OH} \rightleftharpoons \text{NO} + \text{H}_2\text{O}$	1.300E+07	1.900	-950.00
$\text{HNO} + \text{O}_2 \rightleftharpoons \text{HO}_2 + \text{NO}$	1.000E+13	.000	13000.00

Reactions of CN

$\text{CN} + \text{O} \rightleftharpoons \text{CO} + \text{N}$	7.700E+13	.000	.00
$\text{CN} + \text{OH} \rightleftharpoons \text{NCO} + \text{H}$	4.000E+13	.000	.00
$\text{CN} + \text{H}_2\text{O} \rightleftharpoons \text{HCN} + \text{OH}$	8.000E+12	.000	7460.00
$\text{CN} + \text{O}_2 \rightleftharpoons \text{NCO} + \text{O}$	6.140E+12	.000	-440.00
$\text{CN} + \text{H}_2 \rightleftharpoons \text{HCN} + \text{H}$	2.100E+13	.000	4710.00

Reactions of NCO

$\text{NCO} + \text{O} \rightleftharpoons \text{NO} + \text{CO}$	2.350E+13	.000	.00
$\text{NCO} + \text{H} \rightleftharpoons \text{NH} + \text{CO}$	5.400E+13	.000	.00
$\text{NCO} + \text{OH} \rightleftharpoons \text{NO} + \text{H} + \text{CO}$	2.500E+12	.000	.00

NCO+N<=>N ₂ +CO	2.000E+13	.000	.00
NCO+O ₂ <=>NO+CO ₂	2.000E+12	.000	20000.00
NCO+M<=>N+CO+M	8.800E+16	-.500	48000.00
NCO+NO<=>N ₂ O+CO	2.850E+17	-1.520	740.00
NCO+NO<=>N ₂ +CO ₂	5.700E+18	-2.000	800.00

Reactions of HCN

HCN+M<=>H+CN+M	1.040E+29	-3.300	126600.00
HCN+O<=>NCO+H	1.107E+04	2.640	4980.00
HCN+O<=>NH+CO	2.767E+03	2.640	4980.00
HCN+O<=>CN+OH	2.134E+09	1.580	26600.00
HCN+OH<=>HOCN+H	1.100E+06	2.030	13370.00
HCN+OH<=>HNCO+H	4.400E+03	2.260	6400.00
HCN+OH<=>NH ₂ +CO	1.600E+02	2.560	9000.00
HCN+H+M<=>H ₂ CN+M	1.400E+26	-3.400	1900.00

Reactions of HCNN

HCNN+O<=>CO+H+N ₂	2.200E+13	.000	.00
HCNN+O<=>HCN+NO	2.000E+12	.000	.00
HCNN+O ₂ <=>O+HCO+N ₂	1.200E+13	.000	.00
HCNN+OH<=>H+HCO+N ₂	1.200E+13	.000	.00
HCNN+H<=>CH ₂ +N ₂	1.000E+14	.000	.00
H ₂ CN+N<=>N ₂ +CH ₂	6.000E+13	.000	400.00

Reactions of HNCO

HNCO+O<=>NH+CO ₂	9.800E+07	1.410	8500.00
HNCO+O<=>HNO+CO	1.500E+08	1.570	44000.00
HNCO+O<=>NCO+OH	2.200E+06	2.110	11400.00

HNCO+H<=>NH ₂ +CO	2.250E+07	1.700	3800.00
HNCO+H<=>H ₂ +NCO	1.050E+05	2.500	13300.00
HCNO+H<=>H+HNCO	2.100E+15	-.690	2850.00
HCNO+H<=>OH+HCN	2.700E+11	.180	2120.00
HCNO+H<=>NH ₂ +CO	1.700E+14	-.750	2890.00
HOCN+H<=>H+HNCO	2.000E+07	2.000	2000.00
HNCO+OH<=>NCO+H ₂ O	4.650E+12	.000	6850.00
HNCO+OH<=>NH ₂ +CO ₂	1.550E+12	.000	6850.00
HCCO+NO<=>HCNO+CO	2.350E+13	.000	.00

Reactions of NH₃

$\text{NH}_3 + \text{H} \rightleftharpoons \text{NH}_2 + \text{H}_2$	5.400E+05	2.400	9915.00
$\text{NH}_3 + \text{OH} \rightleftharpoons \text{NH}_2 + \text{H}_2\text{O}$	5.000E+07	1.600	955.00
$\text{NH}_3 + \text{O} \rightleftharpoons \text{NH}_2 + \text{OH}$	9.400E+06	1.940	6460.00

Reactions of NO2

$\text{NO} + \text{HO}_2 \rightleftharpoons \text{NO}_2 + \text{OH}$	4.110E+10	.000	-480.00
$\text{NO} + \text{O} + \text{M} \rightleftharpoons \text{NO}_2 + \text{M}$	1.060E+20	-1.410	.00
$\text{NO}_2 + \text{O} \rightleftharpoons \text{NO} + \text{O}_2$	3.900E+12	.000	-
240.00			
$\text{NO}_2 + \text{H} \rightleftharpoons \text{NO} + \text{OH}$	1.320E+14	.000	360.00

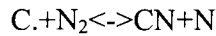
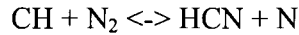
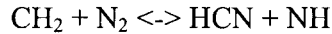
Reactions of NO destruction

$\text{C} + \text{NO} \rightleftharpoons \text{CN} + \text{O}$	1.900E+13	.000	.00
$\text{C} + \text{NO} \rightleftharpoons \text{CO} + \text{N}$	2.900E+13	.000	.00
$\text{CH} + \text{NO} \rightleftharpoons \text{HCN} + \text{O}$	5.000E+13	.000	.00
$\text{CH} + \text{NO} \rightleftharpoons \text{H} + \text{NCO}$	2.000E+13	.000	.00
$\text{CH} + \text{NO} \rightleftharpoons \text{N} + \text{HCO}$	3.000E+13	.000	.00
$\text{CH}_2 + \text{NO} \rightleftharpoons \text{H} + \text{HNCO}$	3.100E+17	-1.380	1270.00
$\text{CH}_2 + \text{NO} \rightleftharpoons \text{OH} + \text{HCN}$	2.900E+14	-.690	760.00
$\text{CH}_2 + \text{NO} \rightleftharpoons \text{H} + \text{HCNO}$	3.800E+13	-.360	580.00
$\text{CH}_2(\text{S}) + \text{NO} \rightleftharpoons \text{H} + \text{HNCO}$	3.100E+17	-1.380	1270.00
$\text{CH}_2(\text{S}) + \text{NO} \rightleftharpoons \text{OH} + \text{HCN}$	2.900E+14	-.690	760.00
$\text{CH}_2(\text{S}) + \text{NO} \rightleftharpoons \text{H} + \text{HCNO}$	3.800E+13	-.360	580.00
$\text{CH}_3 + \text{NO} \rightleftharpoons \text{HCN} + \text{H}_2\text{O}$	9.600E+13	.000	28800.00
$\text{CH}_3 + \text{NO} \rightleftharpoons \text{H}_2\text{CN} + \text{OH}$	1.000E+12	.000	21750.00
$\text{CH}_3 + \text{N} \rightleftharpoons \text{H}_2\text{CN} + \text{H}$	6.100E+14	-.310	290.00
$\text{CH}_3 + \text{N} \rightleftharpoons \text{HCN} + \text{H}_2$	3.700E+12	.150	-90.00

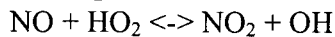
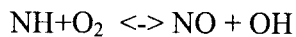
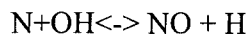
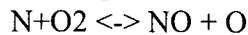
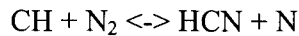
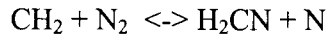
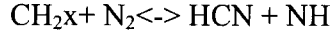
NO_x Formation

NO_x can be formed through three distinctive pathways; thermal pathway generally called Zeldovich Mechanisms, N₂O-intermediate pathway and Prompt NO mechanism [6, 11, 12, 28]. In high temperature flames, Zeldovich Mechanisms is the primary source of NO and NO_x production and is generally considered to be formed in the post-flame gases. This mechanism due to high activation energy of the reaction $\text{O} + \text{N}_2 \rightleftharpoons \text{NO} + \text{O}$ (319,050 kJ/kmol) is unimportant below 1800K temperatures [11,28]. N₂O-intermediate mechanism is recognized to be the major pathway of NO production in lean fuels mixtures [27, 201. According to the sensitivity calculations in low- temperature combustion, Zeldovich mechanism and N₂O-intermediate mechanism are negligible in the overall NO_x production. According to the sensitivity analyses, prompt NO mechanism is the only mechanism, which initiates the NO, and which links NO production to

hydrocarbon chemistry. The hydrocarbon radicals, CH and CH₂ react with molecular nitrogen and form amines or cyano compounds. The amines or cyano compounds are directly responsible for paths leading to the production of NO. The structure of Prompt NO mechanism is:

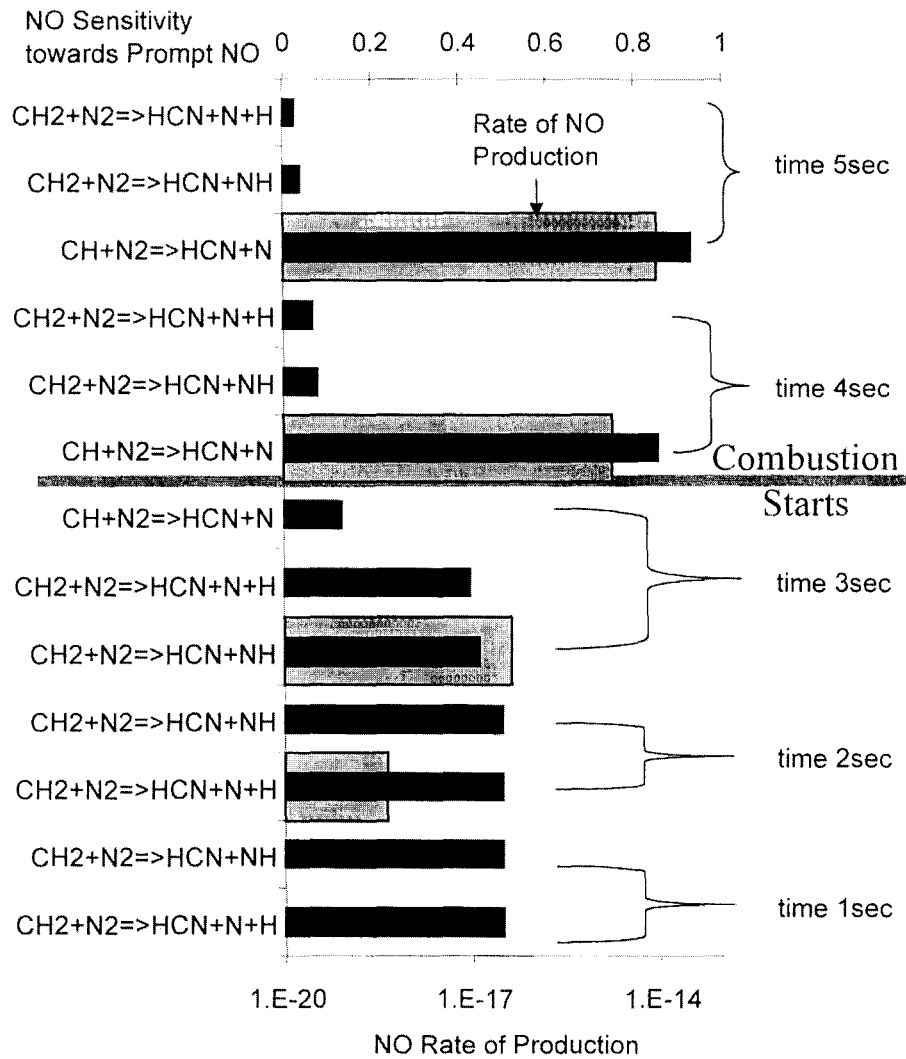


From the sensitivity calculation, the reaction $\text{CH} + \text{N}_2 \rightleftharpoons \text{HCN} + \text{N}$ is the predominant reaction having the most influence on the NO production. CH₂ radical initiates the NO formation process early in the combustion stage; however, its influence slowly loses importance as the combustion proceeds. From the rate of NO production it is evident that CH is the main radical responsible for NO production. As can be seen in Figure 2 the rate of NO production is much higher when $\text{CH} + \text{N}_2 \rightleftharpoons \text{HCN} + \text{N}$ reaction is the dominant. Sensitivity analysis of Prompt NO mechanism towards the production of NO is shown in Figure 2. The sensitivity is calculated for five different time zones where the influence of Prompt NO can be seen and compared to the NO rate of production. At time of 1-3 seconds the CH₂ radical is the principle path through which NO is formed, however, at the time of ignition when methane is rapidly oxidized and when radical production is most active CH becomes the main path leading to NO production. The following Low-Temperature NO_x mechanism suggests the chain-propagating reactions of NO_x production:



These chain-propagating reactions are the only reactions contributing to the total NO_x produced in the system. They are the only reactions directly related to NO formation.

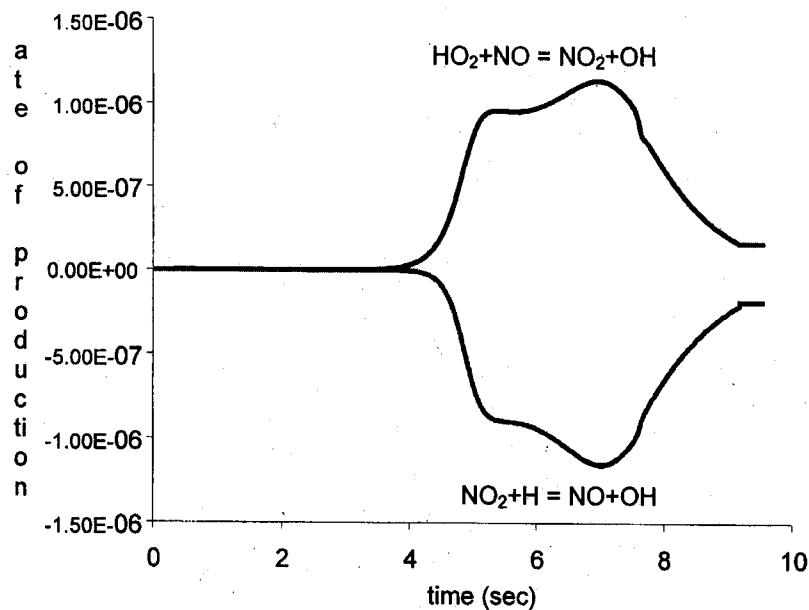
Figure 2



According to the experimental measurements, the overall concentration of NO_x in low temperature combustion was primary composed of NO₂. High concentration of NO₂ recorded during IGT testing can be explained based on the high concentration of HO₂ radical present in combustion. From sensitivity analysis, it is evident, that reaction responsible for the production of

NO_2 is $\text{NO} + \text{HO}_2 \leftrightarrow \text{NO}_2 + \text{OH}$ which is the only reaction contributing to NO_2 production. Also, from the concentration profiles of HO_2 and NO_2 reveal the dependence of HO_2 to NO_2 concentration. This result is in a good agreement with the data presented in [xxx]. Our calculations show that at low temperature combustion HO_2 radicals have long life times, comparing to high temperature combustion. This results in anomalous NO_2 production. The similar situation (unusually high HO_2 concentrations) can happen in turbulent flames, due to turbulent mixing/quenching [xx], which as well leads to overproduction of NO_2 . As can be seen from Figure 3 only two reactions influence NO_2 production or destruction namely $\text{NO} + \text{HO}_2 \leftrightarrow \text{NO}_2 + \text{OH}$ contributing to the entire NO_2 production and $\text{NO}_2 + \text{H} \leftrightarrow \text{NO} + \text{OH}$ contributing to the destruction of NO_2 .

Figure 3



CONCLUSION

A Natural Gas Premixed Forced Internal Recirculation Burner (FIR) decreases NO_x production to sub 10 ppm levels when burning natural gas at low excess air. The burner consists of two stages. In the primary stage a combustion of rich mixture of natural gas and air (air to fuel ratio where varied from 0.37 to 0.69) is effected by specially organized internal recirculation. In secondary stage, air was directed through the primary combustion zone to provide final oxidation of the unburned hydrocarbons. Experimentally measured temperatures in the primary combustion zone were as low as 800K. This design allows reduction NO_x emission levels by lowering the overall combustion temperature. The design also minimizes heat transfer to the cooling water

surrounding the combustion zone and, therefore, is ideal for boilers and process heaters, which presently represent the largest share of natural gas use in the industrial sector. The experiments were conducted on the 5.9 MW watertube boiler. The NO_x emission operations levels were lower than 10 vppm while providing low levels of CO and total hydrocarbon emissions. The NO_x emission consisted of 70 to 80% of NO₂ which differs significantly from NO_x composition in regular burners where NO₂ does not exceed 5% of total NO_x amount.

To explain the low temperature combustion in the first burner stage a detailed chemical mechanism was developed. According to this mechanism, the combustion proceeds through the degenerate chain branching mechanism.

Numerical model assumes that the combustion is initiated by long living radicals and molecules such as CH₃OO, CH₃OOH, etc. due to processes of turbulent mixing and/or recirculation. Calculation results show that adding less than 1 ppm of those molecules ignites methane/oxygen mixture and completes combustion within ms time scale. The calculated characteristic time of oxidation is 50 ms, which is consistent with the gas residence times in the burner. The concentrations of combustion products are within good agreement with the experimentally measured values.

For the explanation of low NO_x emission levels and anomalous NO₂/NO ratios in rich low- temperature flames a detailed chemical NO_x formation mechanism was developed. In rich premixed flames at the temperatures varying from 700 to 1000K, the predicted reaction path of the NO_x formation proceeds through the reactions between molecular nitrogen and CH radicals. Abnormally high NO₂ percentage was explained due to high HO₂ concentration in the flame. The comparison of numerical and experimental results is provided.

Literature

- 1 Smith, D. J., Power Engineering, 1993, (June)
- 2 Castaidini, C., in EPRI/EPA Joint Symposium on Stationary Combustion NO_x Control, Bat Harbour, Florida May 24-27, 1993
- 3 Javier M. Ballester, Cesar Dopazo, Norberto Fueyo, Manuel Hernandez, and Pedro J. Vidal. Fuel 1997 Volume 76 Number 5.
- 4 Paolo Gaffuri, Tiziano Faravelli, Eliseo Ranzi. "Comprehensive Kinetic Model for the Low- Temperature Oxidation of Hydrocarbons", AIChE Journal, May 1997, Vol. 43, No.5
- 5 M. J. Pilling, "Low-temperature Combustion and Autoignition" Volume 35 of series 'Comprehensive Chemical Kinetics', Elsevier, Amsterdam, 1997.
- 6 Glassman Irvin, Combustion, 3rd edition, Academic Press, 1996. Page 83.
- 7 Minkoff G. J., Tipper C. F. H. "Chemistry of Combustion Reactions", London Butterworths, 1962
- 8 Kondratiev V. N., Nikitin E. E. "Kinetika i mehanizm gazopaznyh reaktsii" (in Russian), nauka 1975.

- 9 Vanpee, M., (1956) Sur les reactions associées aux phénomènes de luminescence de la combustion du formaldéhyde. Comptes Rendus, 242, p. 373.
- 10 Vanpee, M., (-I 993) On the Cool Flame of Methane, Combust. Sci. and Tech. 1993. Vol. 93. pp. 363-374.
- 11 Miller A., Bowman C. T., "Mechanism and modeling of nitrogen chemistry in combustion", Prog. Energy Combust. Sci. 1989, Vol. 15, pp287-338
- 12 GRI Mech. 2.11.
- 13 Ruey-Hung Chen, "A Parametric Study of NO₂ Emission from Turbulent H₂ and CH₄ Jet Diffusion Flames", Combustion and Flame, 1998
- 14 Chen, R. -H., and Driscoll, J. F., Twenty-Third Symposium (International) on Combustion, The Combustion Institute, Pittsburgh, 1990, p.281.
- 15 Driscoll, J. F., Chen, R. -H., and Yoon, Y., Combustion and Flame, 88:347 (1987)
- 16 Johnson, G. M., and Smith, M. Y., Combustion Sci. Technol. 19:67 (1978)
- 17 Sano, T., combust. Sci. Technol. 43:259 (1985)
- 18 Hori, M., Matsunaga, N., Malte, P. C., and Marinov, N. M. Twenty-Fourth Symposium (international) on Combustion, The Combustion Institute, Pittsburgh, 1992, p.909.
- 19 GRI MECH 1.2, GRI MECH 2.11
- 20 R.C. Steele, J.H. Tonouchi, D.G. Nicol, D.C. Homing, P.C. Malte, D.T. Pratt; "Characterization of NO_x, N₂O, and CO for Lean-Premixed Combustion in a High-Pressure Jet- Stirred Reactor" Journal of Engineering for Gas Turbines and Power, April 1998. Vol. 120
- 21 Michael Frenklach "A Detailed Kinetic Modeling Study of Aromatics Formation in Laminar Premixed Acetylene and Ethylene Flames" Combustion and Flame 110: 173 - 221 (1997)
- 22 A.KONNOV's detailed reaction mechanism VER 0.4 CHECKED 8/9/98
- 23 REACTION DATABASE FOR CO-C2 COMPOUNDS FILE USABLE BY CHEMKIN 11 (SANDIA) AUTHORS: F. BATTIN-LECLERC AND P. BARBE, 17 MARCH 1997
- 24 The Leeds methane oxidation mechanism
- 25 Linstit <http://chem.leeds.ac.uk/Combustion/Combustion.html>
- 26 V.. Karbach/J.Wamatz; version from July 1, 1997
- 27 R.C. Steele, A.C. Jarret, P.C. Malte, D.G. Nicol; "Variables Affecting NO_x Formation in Lean- Premixed Combustion" Journal of Engineering for Gas Turbines and Power, January 1997. Vol. 119
- 28 Glassman Irvin, Combustion, 3rd edition, Academic Press, 1996. Page 362.
- 29 NIST Standard Reference Database 17, "NIST Chemical Kinetics Database Version 5.0 - Data coverage through 1992" Data and bibliographic citations abstracted and edited by: F.Westley, D.H.Frizzell, J.T.Herron, R.F.Hampson, W.G.Mallard
Database developed by: W.G. Mallard, Chemical Kinetics & Thermodynamics Division - NIST
- 30 CHEMKIN Author: Andy Lutz, Computational Mechanics Division, 8245, Sandia National Laboratories, Livermore, CA, 94550 (415) 294-2761